Effect of Sarcoplasmic Reticulum Calcium Depletion on Intramembranous Charge Movement in Frog Cut Muscle Fibers

DE-SHIEN JONG, PAUL C. PAPE, and W. KNOX CHANDLER

From the Department of Cellular and Molecular Physiology, Yale University School of Medicine, New Haven, Connecticut 06510-8026

ABSTRACT Cut muscle fibers from *Rana temporaria* (sarcomere length, 3.3–3.5 μm; temperature, 13–16°C) were mounted in a double Vaseline-gap chamber and equilibrated for at least an hour with an internal solution that contained 20 mM EGTA and phenol red and an external solution that contained predominantly TEA-gluconate; both solutions were nominally Ca-free. The increase in total myoplasmic concentration of Ca ($\Delta[Ca_T]$) produced by sarcoplasmic reticulum (SR) Ca release was estimated from the change in pH produced when the released Ca was complexed by EGTA (Pape, P. C., D.-S. Jong, and W. K. Chandler. 1995. *Journal of General Physiology.* 106:259–336.). The resting value of SR Ca content, $[Ca_{SR}]_R$ (expressed as myoplasmic concentration), was taken to be equal to the value of $\Delta[Ca_T]$ obtained during a step depolarization (usually to −50 to −40 mV) that was sufficiently long (200–750 ms) to release all of the readily releasable Ca from the SR. In ten fibers, the first depolarization gave $[Ca_{SR}]_R$ = 839–1,698 μM. Progressively smaller values were obtained with subsequent depolarizations until, after 30–40 depolarizations, the value of $[Ca_{SR}]_R$ had usually been reduced to <10 μM. Measurements of intramembranous charge movement, I_{cm}, showed that, as the value of $[Ca_{SR}]_R$ decreased, ON-OFF charge equality held and the amount of charge moved remained constant. ON I_{cm} showed brief initial I_β components and prominent I_γ "humps", even after the value of $[Ca_{SR}]_R$ was <10 μM. Although the amplitude of the hump component decreased during depletion, its duration increased in a manner that preserved the constancy of ON charge. In the depleted state, charge movement was steeply voltage dependent, with a mean value of 7.2 mV for the Boltzmann factor *k*. These and other results are not consistent with the idea that there is one type of charge, Q_β, and that I_γ is a movement of Q_β caused by SR Ca release, as proposed by Pizarro, Csernoch, Uribe, Rodríguez, and Ríos (1991. *Journal of General Physiology.* 97:913–947). Rather, our results imply

Dr. Jong's current address is Department of Animal Science, National Taiwan University, Taipei, Taiwan, R.O.C.

Dr. Pape's current address is Département de Physiologie et Biophysique, Faculté de Médecine, Université de Sherbrooke, Sherbrooke (Québec), Canada J1H5N4.

Address correspondence to Dr. W. K. Chandler, Department of Cellular and Molecular Physiology, Yale University School of Medicine, 333 Cedar Street, New Haven, CT 06510-8026.

J. GEN. PHYSIOL. © The Rockefeller University Press · 0022-1295/95/10/659/46 $2.00
Volume 106 October 1995 659–704

that Q_β and Q_γ represent either two distinct species of charge or two transitions with different properties of a single species of charge, and that SR Ca content or release or some related event alters the kinetics, but not the amount of Q_γ. Many of the properties of Q_γ, as well as the voltage dependence of the rate of SR Ca release for small depolarizations, are consistent with predictions from a simple model in which the voltage sensor for SR Ca release consists of four interacting charge movement particles.

INTRODUCTION

Since intramembranous charge movement was first reported in skeletal muscle (Schneider and Chandler, 1973), considerable interest has been focused on understanding its physiological function. As a result of several studies, as reviewed by Ríos and Pizarro (1991) and Schneider (1994), it is now generally accepted that charge movement plays an important role in the control of sarcoplasmic reticulum (SR) Ca release by the voltage across the membranes of the transverse tubular system. During a step depolarization in a polarized frog muscle fiber, Adrian and Peres (1977, 1979) observed that the charge movement current, I_{cm}, consists of two components, which they called I_β and I_γ. I_β increases rapidly and then decays with an approximately exponential time course whereas, if the depolarization is near or past the mechanical threshold, I_γ shows a delayed "hump". In addition, the charge vs voltage relation is shallow for Q_β and steep for Q_γ. These properties of Q_β and Q_γ have led several investigators to suggest that Q_γ is the component of charge movement that controls SR Ca release in frog skeletal muscle (Almers, 1978; Huang, 1982; Hui, 1983; Vergara and Caputo, 1983; Melzer, Schneider, Simon, and Szucs, 1986; Hui and Chandler, 1990, 1991). The situation may be different in mammalian skeletal muscle, however, where I_γ humps are usually not observed (Ríos and Pizarro, 1991). A possible explanation for the occurrence of SR Ca release in fibers without I_γ humps is given in the Discussion.

In a recent series of experiments carried out on frog cut muscle fibers, SR Ca content or release or some related event was shown to alter the time course of charge movement current under certain conditions (Csernoch, Pizarro, Uribe, Rodríguez, and Ríos, 1991; García, Pizarro, Ríos, and Stefani, 1991; Szucs, Csernoch, Magyar, and Kovács, 1991; Pizarro, Csernoch, Uribe, Rodríguez, and Ríos, 1991). Pizarro et al. (1991) developed an explanation for these kinetic changes based on an idea first proposed by one of us as a possible explanation of I_γ humps (W. K. Chandler, quoted in Horowicz and Schneider, 1981). When Ca moves from the SR into the myoplasm, free [Ca] is elevated in the space between the membranes of the transverse tubules and the SR. As a result, calcium binds to the sarcoplasmic surface of the tubular membrane and produces a change in surface potential. If the potential between the internal and external solutions is unchanged, as would be expected during a voltage-clamp experiment, an equal but opposite change in potential must develop across the tubular membrane, and this would favor the movement of additional charge.

According to the proposal of Pizarro et al. (1991), frog skeletal muscle has only one kind of intramembranous charged particle that is involved in excitation-contraction coupling and this particle has the properties usually associated with Q_β.

The Q_β particles distribute between two states, resting and activating, and transitions from one state to the other occur according to rate constants that are functions of the potential across the tubular membrane. The distribution of particles between the two states satisfies the Boltzmann distribution so that the equilibrium amount of charge, Q, is given by

$$Q = \frac{Q_{max}}{1 + \exp[-(V - \bar{V})/k]}. \quad (1)$$

Q_{max} represents the maximal amount of charge. V represents the voltage measured between the internal and external solutions, which is equal to the sum of the potential across the tubular membrane and the surface potentials on both sides of the membranes. $\bar{V}$ is the value of V at which the amount of equilibrium charge in the resting and activating states is the same, and k is a voltage steepness factor. In the calculations described by Pizarro et al. (1991), the value of k was 11–15 mV.

During a step depolarization, in the absence of SR Ca release, the surface potential at the sarcoplasmic surface of the tubular membrane (as well as that at the luminal surface) is expected to remain constant. Thus, a step change in V would be expected to produce a step change in voltage directly across the tubular membrane. Consequently, the forward and backward rate constants for transitions of Q_β between the resting and activating states would be expected to be constant and, as a result, the current from charge movement would be expected to have an exponential time course. On the other hand, if SR Ca release were able to occur after a step change in V, the proposed change in surface potential and the associated change in membrane potential would shift the Q_β vs V relation to more negative potentials and favor the movement of additional Q_β charge. According to Pizarro et al. (1991), Q_γ is this additional component of Q_β charge that is caused by SR Ca release.

If these ideas about the origin of Q_γ in frog skeletal muscle are correct, three simple predictions follow about the properties of charge movement currents that would be observed if the SR were depleted of all of its readily releasable Ca. (*a*) The time course of ON I_{cm} should resemble that of I_β; it should be approximately exponential at all voltages and should not show I_γ humps. (*b*) The OFF I_{cm} should have an exponential time course with a time constant that is independent of both the voltage of the pulse and its duration. (*c*) The charge (Q_{cm}) vs V relation should obey Eq. 1 with a value of k that is appropriate for Q_β, 11–15 mV.

This article describes experiments that were designed to test these predictions. Frog cut muscle fibers were depleted of Ca by equilibration with Ca-free internal and external solutions. The internal solution contained 20 mM EGTA. The external solution contained gluconate as the predominant anion so that the proportion of total charge that has the properties associated with Q_γ would be as large as possible (Chen and Hui, 1991). After an equilibration period of at least an hour, successive step depolarizations were used to deplete the SR of any remaining Ca. After 30–40 such depolarizations, the amount of readily releasable Ca inside the SR was usually <10 μM. Contrary to prediction *a*, prominent I_γ humps were always observed in Ca-depleted fibers. Contrary to prediction *b*, the time course of OFF I_{cm} varied with the amplitude and the duration of a pulse. Contrary to prediction *c*, the

mean value of k in a Ca-depleted fiber, estimated from a least-squares fit of Eq. 1 to the Q_{cm} vs V data, was 7 mV, similar to that obtained previously from fibers not depleted of Ca.

These results show clearly that the Q_γ component of intramembranous charge in frog muscle does not require the presence of Ca inside either the SR or the myoplasm nor does it require Ca flux through SR Ca channels. Thus, SR Ca content or release or some related event does not fundamentally cause Q_γ. On the other hand, our results do show that SR Ca, in amounts as small as tens of micromolar, can alter the ON kinetics of Q_γ in a manner that provides positive feedback between Ca release and Q_γ. Although the underlying mechanism for this effect remains unclear, the last section of the Discussion presents a plausible explanation: the change in kinetics of Q_γ might be caused by a shift in the Q_γ vs V relation produced by a change in surface potential, analogous to the idea proposed by Pizarro et al. (1991) to explain the origin of Q_γ in terms of a shift in the Q_β vs V relation. Whatever the correct explanation for the effect of SR Ca on the ON kinetics of Q_γ, however, we believe that many of the previous experimental results that were attributed to a shift in the Q_β vs V relation produced by changes in surface potential (Csernoch et al., 1991; García et al. 1991; Szucs et al., 1991; Pizarro et al., 1991) can reasonably be attributed to this change in the kinetics of Q_γ.

Since the experiments in this article describe, for the first time, intramembranous charge movement in Ca-depleted fibers, they provide an opportunity to compare experimental results, unaltered by any effects of SR Ca, with predictions from theoretical models of charge movement. The Discussion and Appendix describe comparisons that were made with the models proposed by Huang (1984) and by Ríos, Karhanek, Ma, and González (1993). Each model, in its original form, fails in a major way to describe certain experimental results.

Several other models, based on four interacting charge movement particles, were investigated and one of these is described in the Discussion. With appropriate selection of parameters, the model is able to provide a good fit to the steady state Q_{cm} vs V data and to generate pronounced ON I_γ humps. With the same parameters, the model explains, qualitatively, the main effects of pulse amplitude and duration on the time course of OFF I_{cm}. On the assumption that the four interacting particles serve as the voltage sensor for SR Ca release, the model also predicts the voltage dependence of the rate of release that has been observed during small depolarizations in fibers studied under similar conditions but with millimolar amounts of Ca inside the SR (Pape, Jong, and Chandler, 1995).

A preliminary report of some of these results has been presented to the Biophysical Society (Jong, Pape, and Chandler, 1992).

METHODS

Cut muscle fibers (Hille and Campbell, 1976) from cold-adapted *Rana temporaria* were stretched to a sarcomere length of 3.3–3.5 μm and mounted in a double Vaseline-gap chamber (Kovács, Ríos, and Schneider, 1983; Irving, Maylie, Sizto, and Chandler, 1987). The end-pool segments of the fiber were permeabilized by a 2-min exposure to an end-pool solution with 0.01% saponin followed by a thorough rinse with a saponin-free end-pool solution. The composition of the end-pool solution was 45 mM Cs-glutamate, 20 mM Cs_2EGTA, 6.8 mM $MgSO_4$, 5.5 mM Cs_2-ATP, 20

mM Cs_2-creatine phosphate, 5 mM Cs_5-phospho(enol)pyruvate, and 5 mM 3-[*N*-Morpholino]-propanesulfonic acid (MOPS); the pH was adjusted to 7.0 by the addition of CsOH and the calculated concentration of free Mg was 1 mM (Pape et al., 1995). The composition of the central-pool solution was 110 mM TEA-gluconate, 10 mM $MgSO_4$, 1 μM tetrodotoxin, and 10 mM MOPS, pH = 7.1. Except for the latter part of the experiment in Fig. 4 (see text and figure legend), both internal and external solutions were nominally Ca-free. The temperature was 13–16°C and the holding potential measured in end pool 1 was −90 mV.

The experimental methods are the same as those used previously in this laboratory. The optical apparatus is described in Irving et al. (1987). SR Ca release was estimated with the EGTA-phenol red method, as described in Pape et al. (1995). With the concentration used in the end-pool solutions, 20 mM, EGTA is expected to capture almost all of the Ca released from the SR within <0.1 ms and to exchange it rapidly for protons with a 1:2 stoichiometry. The accompanying change in myoplasmic pH, ΔpH, is measured with phenol red and the change in total myoplasmic Ca concentration, $\Delta[Ca_T]$, is determined from the equation $\Delta[Ca_T] = -(\beta/2)\Delta pH$, in which β represents the buffering power of myoplasm, 22 mM/pH unit. The electrical methods used for the measurement of intramembranous charge movement are described in Chandler and Hui (1990) and in Hui and Chandler (1990, 1991).

Several parameters were monitored routinely during the course of the experiments: fiber diameter, holding current, apparent capacitance (C_{app}), internal longitudinal resistance per unit length of fiber (r_i), capacitance of the surface (including tubular) membranes per unit length of fiber (c_m), concentration of phenol red, resting pH (pH_R), and the amount of readily releasable Ca inside the SR expressed as myoplasmic concentration ($[Ca_{SR}]_R$).

Statistical Tests of Significance

The difference between the mean values of two sets of results was assessed with Student's two-tailed *t* test and considered to be significant if $P < 0.05$.

In experiments such as the one illustrated in Fig. 3 *B* (see also columns 6 and 7 of Table I), a sloping straight line was least-squares fitted to values of Q_{cm} plotted against time (fits not shown). The test described on page 265 in Pape et al. (1995) was used to determine whether the value of the slope of the line was significantly different from zero.

In Fig. 8 *B*, the experimental values of y_i (−OFF Q_{cm}) at different values of x_i (ON Q_{cm}) were least-squares fitted by a sloping straight line that was constrained to go through the origin. The formula for a line that is constrained to pass through the point $x = x_0$, $y = y_0$ can be written

$$Y = y_0 + b(X - x_0), \tag{2}$$

in which *b* is the slope of the line. In Fig. 8 *B*, Student's two-tailed *t* test was used to determine whether the value of *b* was significantly different from 1. For this purpose, the residual variance of *y*, denoted by var(*y*), for *n* values of y_i was estimated from

$$\text{var}(y) = \frac{\Sigma (y_i - Y)^2}{(n-1)}. \tag{3}$$

The variance of *b*, denoted by var(*b*), was calculated from

$$\text{var}(b) = \frac{\text{var}(y)}{\Sigma (x_i - x_0)^2}, \tag{4}$$

with $x_0 = 0$ (see chapter 12 in Colquhoun, 1971). The value of *b* was considered to be significantly different from 1 if the value of *P* determined with Student's two-tailed *t* test was <0.05. For this test, the value of *t* was set equal to $(b - 1)/\sqrt{\text{var}(b)}$.

RESULTS

In the experiments described in this article, SR Ca release and intramembranous charge movement were measured simultaneously in 10 cut fibers that had been equilibrated with internal and external solutions that were nominally Ca-free. The first depolarization, a 200–750 ms pulse to −50 to −30 mV, was applied after a 57–78-min period of equilibration. It increased the total concentration of Ca in the myoplasmic solution, $\Delta[Ca_T]$, by 839–1,698 μM. The second depolarization, applied 1–3 min later, increased $\Delta[Ca_T]$ by 414–898 μM. Because the amplitude and duration of these depolarizations were sufficient for $\Delta[Ca_T]$ to reach a plateau level, these values of $\Delta[Ca_T]$ are taken to represent $[Ca_{SR}]_R$, the amount of readily releasable Ca inside the SR just before the depolarization. After 30–40 such depolarizations applied every 1–2 min, the value of $[Ca_{SR}]_R$ became very small, usually <10 μM. Important factors in the achievement of such marked Ca depletion in our experiments were the presence of a large concentration of EGTA in the internal solution and the absence of Ca from both the external and internal solutions. This article describes results obtained from measurements made during the second and subsequent depolarizations.

Intramembranous Charge Movement during a Depolarization to −40 mV in a Fiber Partially Depleted of Ca

Fig. 1 shows records obtained during the third depolarization of a fiber that had been equilibrated for over an hour with Ca-free internal and external solutions. The holding potential was −90 mV and the potential during the 200-ms pulse was −40 mV.

The top trace in Fig. 1 shows V_1, the voltage measured in end pool 1. The middle trace shows $I_{test} - I_{control}$. I_{test} represents the current recorded during the pulse to −40 mV. $I_{control}$ was constructed for the same voltage excursion from the average of eight current records taken during control potential steps from −110 to −90 mV,

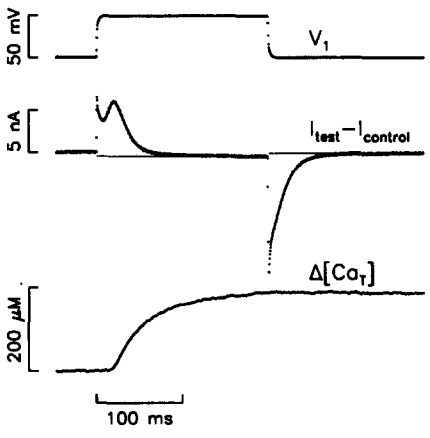

FIGURE 1. Intramembranous charge movement currents and SR Ca release during and after a 200-ms depolarization to −40 mV in a fiber partially depleted of Ca. The top trace shows V_1. The middle trace shows $I_{test} - I_{control}$. The steady levels during and after the pulse, −0.48 and −0.11 nA, respectively, were estimated from the mean values of the corresponding segments of the trace during the final 7.2 ms; these are indicated by thin horizontal lines. The bottom trace shows $\Delta[Ca_T]$. Fiber reference, N28901; time after saponin treatment, 80 min; sarcomere length, 3.4 μm; fiber diameter, 151 μm; holding current, −47 nA; C_{app}, 0.01158 μF; r_i, 2.36 MΩ/cm; c_m, 0.156 μF/cm; concentration of phenol red at the optical site, 1.068 mM; pH_R, 6.837; temperature, 14°C; interval of time between data points, 0.36 ms.

applied just before the test pulse, as described in Hui and Chandler (1990). $I_{test} - I_{control}$ is expected to be composed of current from intramembranous charge movement plus a small ionic component if the ionic current vs voltage curve is nonlinear between −110 and −40 mV. The mean values of current during the final 7.2 ms segments during and after the pulse were used to estimate the steady state values of the ON and OFF ionic components, respectively. These are indicated by two thin horizontal lines. Here, and throughout this article, the values of the ionic component at other times are assumed to be given by the steady state values rounded according to the normalized voltage template (Hui and Chandler, 1990). The difference between $I_{test} - I_{control}$ and the ionic component is taken to represent I_{cm}, the current from intramembranous charge movement.

After depolarization, I_{cm} showed an initial rapid increase followed by a dip and then a second transient increase. These early and late components of current were first described by Adrian and Peres (1977, 1979), who called them I_β and I_γ, respectively. In the experiments described in this article, the charge associated with I_β appeared to be much smaller than that associated with I_γ, owing to the use of gluconate in the external solution (Chen and Hui, 1991). In Fig. 1, the initial time course of I_β appears to follow a decreasing exponential function, at least to a first approximation, whereas the time course of I_γ has a delayed hump. After the decay of these two components, ON I_{cm} was relatively constant and, in particular, did not have a negative phase, as has been observed by Pizarro et al. (1991) and Shirokova, Pizarro, and Ríos (1994) (see Discussion). After repolarization, $I_{test} - I_{control}$ rapidly reached a negative peak and then decayed to the horizontal line, which has a value that is close to that of the prestimulus baseline.

The bottom trace in Fig. 1 shows $\Delta[Ca_T]$, as estimated with the EGTA-phenol red method (Pape et al., 1995). The plateau value at the end of the pulse is taken to represent $[Ca_{SR}]_R$. Its value, 188 μM, is much smaller than the mean value of $[Ca_{SR}]_R$ obtained in similar experiments on fibers equilibrated with an end-pool solution that contained 20 mM EGTA plus 1.76 mM Ca, 2,544 μM (Pape et al., 1995).

Intramembranous Charge Movement with Different Values of $[Ca_{SR}]_R$

Fig. 2 shows sets of four superimposed traces taken at different times during SR Ca depletion, from the fiber used in Fig. 1. Numbers 1–4 denote, in sequence, traces obtained during the 2nd, 3rd, 10th, and 28th stimulations; the traces labeled 2 are the same as those in Fig. 1. According to the plateau values of $\Delta[Ca_T]$ (*bottom traces*), $[Ca_{SR}]_R$ = 414 μM in trace 1, 188 μM in trace 2, 58 μM in trace 3, and 4 μM in trace 4.

The middle set of records in Fig. 2 shows I_{cm}. Each trace was obtained by subtraction of the ionic components from the ON and OFF segments of $I_{test} - I_{control}$, as described above in connection with Fig. 1. The four superimposed ON traces have similar early I_β components but different I_γ humps. As the experiment progressed and the value of $[Ca_{SR}]_R$ became smaller, the peak value of the I_γ hump decreased and its duration increased. Even after the SR had been markedly depleted of Ca, I_β and I_γ components were clearly discernible (trace 4) and, at −30 and −20 mV, I_γ humps were pronounced (see Fig. 5 *A* below).

After repolarization, the four traces of OFF I_{cm} were nearly identical. Because each of the preceding pulses had released almost all of the readily releasable Ca

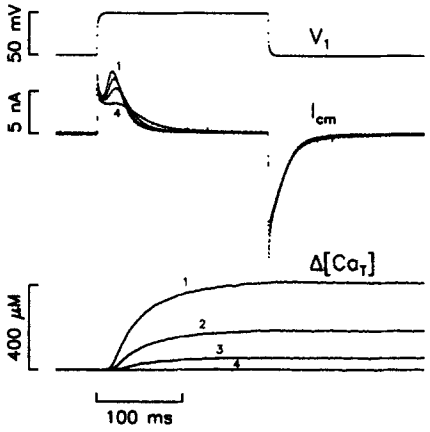

FIGURE 2. Effect of SR Ca depletion on currents from intramembranous charge movement during and after a 200-ms depolarization to −40 mV. Traces from four runs from the fiber used for Fig. 1 are shown superimposed. The top traces show V_1. The middle traces show I_{cm}, obtained from the $I_{test} - I_{control}$ traces by subtraction of the ionic components, as described in the text. The peak value of the I_γ hump progressively decreased as the SR Ca content decreased. The bottom traces show $\Delta[Ca_T]$. Numbers 1–4 refer, respectively, to traces obtained with the 2nd, 3rd, 10th, and 28th stimulations; the traces labeled 2 are the same as those shown in Fig. 1. First and last values: time after saponin treatment, 79–115 min; holding current, −47 and −50 nA; C_{app}, 0.01158–0.01153 μF; r_i, 2.37–2.28 MΩ/cm; c_m, 0.155–0.155 μF/cm; concentration of phenol red at the optical site, 1.055–1.392 mM; pH_R, 6.850–6.866. Additional information is given in the legend of Fig. 1.

from the SR into the myoplasm, where it could become complexed by EGTA, it is important to assess the changes in myoplasmic free [Ca] that had occurred at the time of repolarization. According to Pape et al. (1995), any gradients of freely diffusible EGTA and CaEGTA that develop within the myofibril during SR Ca release should dissipate within ~10 ms after SR Ca release is completed. Consequently, the values of [EGTA] and [CaEGTA], and consequently the value of free [Ca] (given by [CaEGTA]/[EGTA] times K_{Dapp}, the apparent dissociation constant of CaEGTA), should have been essentially constant throughout the myofibril at the time of repolarization.

In Fig. 2, the largest change in [CaEGTA] occurred during trace 1 when [CaEGTA] increased by 414 μM. Concomitantly, the value of myoplasmic pH decreased by 0.038 pH units (Eq. A7 in Pape et al., 1995, with a value of 22 mM/pH unit for the buffering power of myoplasm), from a resting value of 6.850 to 6.812. At pH 6.812, K_{Dapp} = 0.889 μM (calculated from Eq. A9 in Pape et al., 1995, with the parameters given in that article). If the equilibration period of the fiber with Ca-free solutions had been sufficient to reduce the resting value of [CaEGTA] to zero, the resting value of free [Ca] would also have been zero. By the end of the pulse when repolarization occurred, the value of [CaEGTA] would have been 414 μM and, if the resting value of [EGTA] had been 20 mM, the value of [EGTA] would have been 19,586 μM, which gives a value of 0.019 μM for [Ca] (K_{Dapp} = 0.889 μM). Thus, the nearly identical OFF I_{cm} traces in Fig. 2 indicate that the OFF kinetics of I_{cm} is insensitive to changes in myoplasmic free [Ca] in the range between 0 and ~0.02 μM.

The traces of ON and OFF I_{cm} in Fig. 2 are typical of those observed in all of our experiments in which the value of $[Ca_{SR}]_R$ was reduced from 414–898 to <10 μM. Two observations make it likely that the progressive changes in the time course of

ON I_{cm} from traces 1 to 4 are due to SR Ca depletion rather than fiber run down or some other factor associated with the duration of the experiment: (*a*) similar changes were not observed in other experiments of similar duration in which 1.76 mM Ca was present in the end-pool solutions and the SR Ca content remained relatively constant (not shown) and (*b*) the changes could be reversed by the addition of Ca to the end-pool solutions (see Fig. 4 below).

Fig. 3 *A* shows the values of $[Ca_{SR}]_R$ in this experiment, plotted as a function of time after saponin treatment. With some scatter, the values of $[Ca_{SR}]_R$ progressively decreased during the course of the experiment and became <10 μM after 110 min. Most of the scatter is probably due to different periods of recovery between successive stimulations, which allowed different amounts of Ca to be reaccumulated by the SR.

Fig. 3 *B* shows the absolute values of ON (*open circles*) and OFF (*filled circles*) charge obtained by integration of traces of I_{cm} such as those shown in Fig. 2. Even though the time course of ON I_{cm}, especially the I_γ component, changed considerably during the course of the experiment (Fig. 2), the amounts of ON and OFF charge remained relatively constant and approximately equal to each other.

The Effect of SR Ca Depletion on ON I_{cm} Is Reversible

Two experiments were carried out to find out whether the reduction in the amplitude of the I_γ hump that is associated with SR Ca depletion is reversible. Fig. 4 shows traces from one of these experiments. The top trace shows V_1 associated with

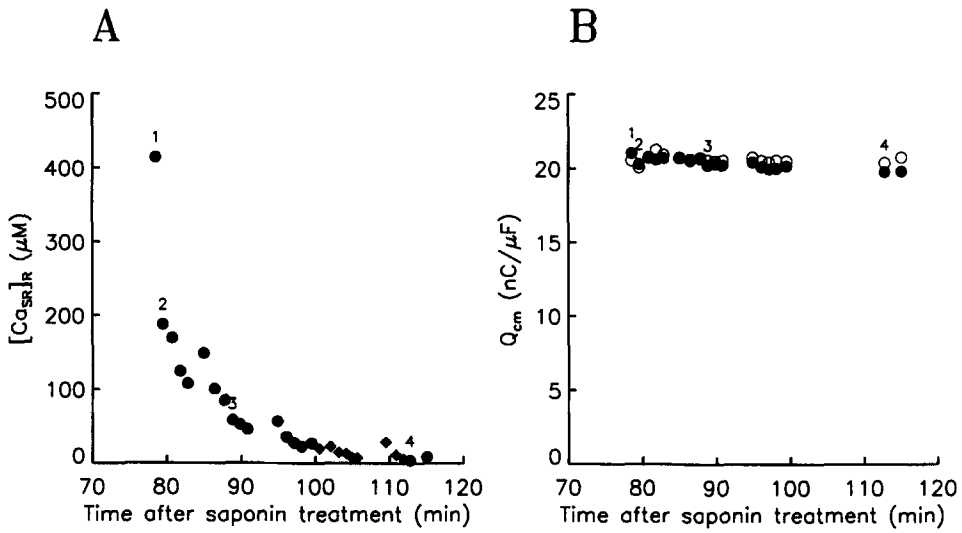

FIGURE 3. Values of $[Ca_{SR}]_R$ (*A*) and Q_{cm} (*B*) plotted as a function of time after saponin treatment, from the experiment illustrated in Figs. 1 and 2. (*A*) Each value of $[Ca_{SR}]_R$ was taken from the final value of $\Delta[Ca_T]$ that was reached during a 200-ms pulse to −40 mV (*circles*) or −20 mV (*diamonds*). (*B*) Open and filled circles denote the absolute values of ON and OFF Q_{cm}, respectively, associated with a pulse to −40 mV. Numbers 1–4 mark points associated with the corresponding traces in Fig. 2. Additional information is given in the legends of Figs. 1 and 2.

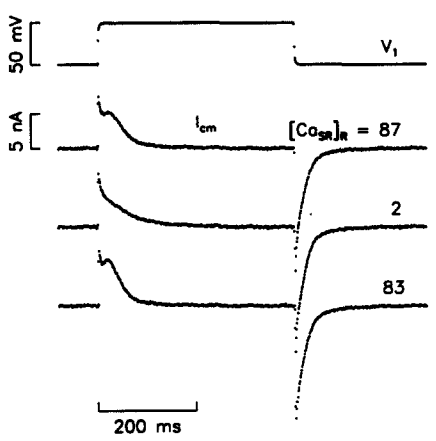

FIGURE 4. Reversibility of the effects of SR Ca depletion on I_{cm}. V_1 and three I_{cm} traces taken, from top to bottom, 80, 116, and 149 min after saponin treatment with $[Ca_{SR}]_R$ = 87, 2, and 83 μM, as indicated. The end-pool solution contained 0 mM Ca until 131 min after saponin treatment when 1.76 mM Ca was added. Fiber reference, D17902; sarcomere length, 3.4 μm; temperature, 14°C; interval of time between data points, 0.96 ms. First and last values: fiber diameter, 119–109 μm; holding current, −49 to −55 nA; C_{app}, 0.01924–0.01930 μF; r_i, 1.96–2.24 MΩ/cm; c_m, 0.261–0.257 μF/cm; concentration of phenol red at the optical site, 1.578–2.608 mM; pH_R, 6.788–6.792.

a 400-ms pulse to −40 mV. The second trace shows I_{cm} associated with the 22nd such depolarization, when $[Ca_{SR}]_R$ = 87 μM, as indicated on the trace. I_β and I_γ components are apparent. The third trace, taken later in the experiment when $[Ca_{SR}]_R$ = 2 μM, shows that the amplitude of the I_γ hump had been reduced and its duration prolonged. 15 min after this trace was taken, 1.76 mM Ca was added to the end-pool solutions. The bottom trace, taken 18 min after Ca addition when $[Ca_{SR}]_R$ = 83 μM, shows that a prominent I_γ hump had returned.

In these three I_{cm} traces, the early I_β components are essentially the same as are the OFF segments. The values of ON and OFF Q_{cm} are also similar: from top to bottom, ON Q_{cm} = 17.7, 17.5, and 18.7 nC/μF and OFF Q_{cm} = −19.1, −18.9, and −21.0 nC/μF. In this experiment, the main effect of SR Ca depletion appears to have been on the time course of I_γ, as observed in the experiment in Fig. 2.

In Fig. 4, the I_γ hump in the bottom trace (labeled 83) is somewhat more pronounced than that in the second trace (labeled 87), although the values of $[Ca_{SR}]_R$ were similar. This difference in I_γ is probably due to the fact that $[Ca_{SR}]_R$ was measured at the optical site in the middle of the fiber in the central-pool region whereas I_{cm} was measured along the entire length of the fiber in the central-pool region and included contributions from membranes under the Vaseline seals (Chandler and Hui, 1990; Hui and Chandler, 1990). When the trace with $[Ca_{SR}]_R$ = 87 μM was taken, the fiber had been equilibrated with Ca-free solutions in the end pools and in the central pool for 80 min, and 21 pulses had been applied previously to reduce $[Ca_{SR}]_R$. The values of myoplasmic free [Ca] and $[Ca_{SR}]_R$ would be expected to have been uniformly small throughout the fiber, with maximal values at the optical site because the end-pool solutions were Ca-free. On the other hand, when the trace with $[Ca_{SR}]_R$ = 83 μM was taken, 1.76 mM Ca had been present in the end-pool solutions for only 18 min. Consequently, gradients of myoplasmic free [Ca] and $[Ca_{SR}]_R$ may have been present, with minimal values at the optical site. Thus, although the two traces were associated with similar values of $[Ca_{SR}]_R$ at the optical site, the mean value of $[Ca_{SR}]_R$ along the fiber was probably smaller when the 87 μM trace was taken than when the 83 μM trace was taken. Such a difference would explain the more pronounced I_γ hump in the 83 μM trace.

The general conclusion from this and the other similar experiment (not shown) is that the change in ON I_{cm} produced by SR Ca depletion is reversible.

Equality and Constancy of ON and OFF Charge During SR Ca Depletion

One of the important questions that arises in the study of intramembranous charge movement is whether the amounts of ON and OFF charge are equal. In most studies that address this point in frog muscle, ON-OFF charge equality has been found (for example, Schneider and Chandler, 1973; Adrian and Almers, 1976; Chandler, Rakowski and Schneider, 1976; Huang, 1983; Melzer et al., 1986; Huang, 1994*a*). Under certain conditions, however, when Ca is released from the SR, the amount of ON charge has been reported to exceed that of OFF charge (Csernoch et al., 1991; García et al., 1991; Szucs et al., 1991). It was therefore important to find out whether ON-OFF charge equality held in our experiments. To determine this, the data shown in Fig. 3 *B* and similar data from nine other fibers were subjected to three statistical tests.

The first test was to add the values of ON and OFF Q_{cm} (with their respective positive and negative signs) for individual pulses and to determine the mean value of ON plus OFF Q_{cm} for each fiber. If ON-OFF charge equality holds, the absolute values of ON and OFF Q_{cm} for each pulse would be the same and the value of ON plus OFF Q_{cm} would be zero. The results of this test are given in Table I. The first four columns give fiber references, pulse potentials, times after saponin treatment, and initial (maximal) values of $[Ca_{SR}]_R$. Column 5 gives the mean values of ON Q_{cm}, each determined from 10–35 measurements on the same fiber. Column 6 gives the mean values of ON plus OFF Q_{cm}. 9 of the 10 values are marked by an asterisk to indicate that they are significantly different from zero. Although each of these values might be taken as evidence of ON-OFF charge inequality in a particular fiber, the mean value from all of the fibers, -1.07 nC/μF, is not significantly different from zero. Thus, there is no consistent difference between the amounts of ON and OFF charge in different fibers. Within the accuracy of our measurements, the ON-OFF charge inequality in each fiber can be reasonably attributed to a consistent inaccuracy in the measurement of ON or OFF Q_{cm} in that fiber. The source of this inaccuracy appears to vary from fiber to fiber so that, when the values from different fibers are averaged, ON-OFF charge equality appears to hold, at least at potentials between -50 and -40 mV. This result is different from that reported in the same range of potentials by Csernoch et al. (1991), García et al. (1991), and Szucs et al. (1991), who found that the absolute value of ON Q_{cm} exceeded that of OFF Q_{cm} by 1–4 nC/μF.

The second and third tests involved fitting the values of ON and OFF Q_{cm} plotted against time (Fig. 3 *B*) with sloping straight lines (not shown). Columns 7 and 8 give the values of the slopes of the lines for ON and OFF Q_{cm}, respectively. Values that are significantly different from zero are marked by an asterisk. Although 8 of the 10 ON slopes and 2 of the 10 OFF slopes are significantly different from zero, their respective mean values, -0.0117 and -0.0032 nC/(μF·min), are not. For reasons similar to those given in the preceding paragraph, these results are consistent with the idea that the values of ON and OFF Q_{cm} do not depend on the value of $[Ca_{SR}]_R$, at least under the conditions used for the experiments in Table I.

TABLE I

ON and OFF Q_{cm} during SR Ca Depletion

(1) Fiber	(2) V_1	(3) Time after saponin	(4) $[Ca_{SR}]_R$	(5) ON Q_{cm}	(6) ON + OFF Q_{cm}	(7) ON Q_{cm} vs time	(8) OFF Q_{cm} vs time
	mV	*min*	*μM*	*nC/μF*	*nC/μF*	*nC/(μF·min)*	*nC/(μF·min)*
N28901	−40	79–115	414	20.36	−0.26*	−0.0292*	0.0037
D17902	−40	60–116	619	17.77	−1.49*	−0.0049*	−0.0001
416911	−45	59–111	787	15.79	2.38*	−0.0435*	0.0110
918911	−45	70–144	741	19.31	0.56*	0.0247*	−0.0235*
O17911	−45	80–142	759	19.15	−0.81*	−0.0343*	−0.0013
O31911	−45	72–120	641	17.10	−0.86*	0.0109*	−0.0119
N05911	−45	68–129	880	15.56	−6.97*	0.0253	0.0056
N06911	−45	72–124	898	17.08	−1.38*	0.0374*	−0.0363*
N07911	−50	65–126	866	14.01	0.09	−0.0997*	0.0095
N08911	−50	76–133	619	15.71	−2.00*	−0.0040	0.0116
Mean					−1.07	−0.0117	−0.0032
SEM					0.76	0.0130	0.0051

Columns 1 and 2 give the fiber references and the values of the voltage during the pulse; pulse durations varied from 200 to 750 ms. Column 3 gives the initial and final values of the time after saponin treatment. Column 4 gives the initial value of $[Ca_{SR}]_R$. Column 5 gives the mean value of ON Q_{cm} obtained from each fiber. Column 6 gives the mean value of the sum of ON and OFF Q_{cm} from each fiber; a positive (negative) number means that the absolute value of ON (OFF) charge was greater than that for OFF (ON) charge. Columns 7 and 8 give the values of the slope of a straight line that was least-squares fitted to the values of ON Q_{cm} and OFF Q_{cm}, respectively, plotted as a function of time after saponin treatment of the end-pool segments. Each of the values in columns 5–8 was determined from 10–35 measurements. In columns 6–8, an asterisk denotes values that are significantly different from zero. Sarcomere length, 3.3–3.5 μm; fiber diameter, 92–158 μm; holding current, −27 to −58 nA; r_i, 1.58–2.61 MΩ/cm; c_m, 0.155–0.308 μF/cm; concentration of phenol red at the optical site, 0.615–2.135 mM; pH_R, 6.705–6.922 μM; temperature, 13–16°C. Since charge movement records from the first depolarization were not used in these experiments, the initial values are those associated with the second depolarization.

Two conclusions follow from the results in Figs. 1–3 and Table I. Firstly, within the accuracy of our measurements, ON-OFF charge equality holds for pulse potentials between −50 and −40 mV, at least when the value of $[Ca_{SR}]_R$ is no more than several hundred micromolar and the duration of the pulse is sufficiently long to deplete the SR of almost all of its readily releasable Ca. Secondly, the value of ON or OFF Q_{cm} remains essentially constant when the value of $[Ca_{SR}]_R$ is reduced from 414–898 to <10 μM.

After SR Ca Depletion, Pronounced I_γ Humps Can Be Elicited

After the fiber used for Figs. 1–3 had its SR depleted of essentially all of its readily releasable Ca, I_{cm} was measured with pulses to different voltages. Six of these traces are shown in Fig. 5 *A*, with voltages indicated (in millivolts). I_γ humps are apparent at $V_1 \geq -44$ mV and are especially pronounced at −30 and −20 mV. Although the values of $d\Delta[Ca_T]/dt$ and $\Delta[Ca]$ (the change in spatially averaged myoplasmic free [Ca]) were not resolvable (not shown), they were clearly <0.05 μM/ms and <1 nM, respectively.

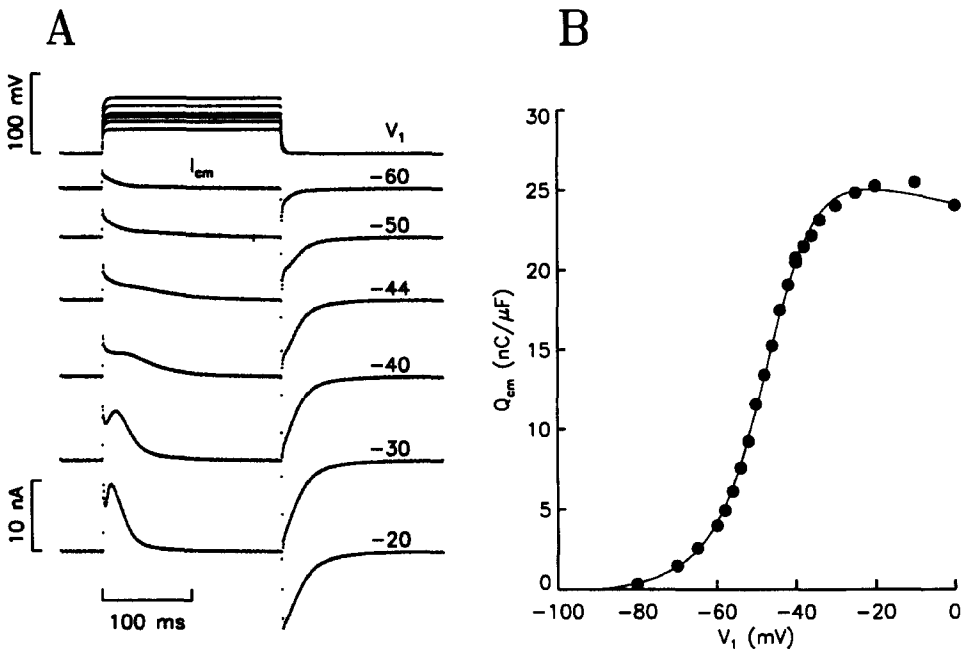

FIGURE 5. Voltage dependence of intramembranous charge movement after SR Ca depletion. (*A*) The top superimposed traces show V_1. The next six traces show I_{cm} at the indicated values of voltage (in millivolts). (*B*) Values of OFF Q_{cm} plotted as a function of V_1. The theoretical curve represents a least-squares fit of Eq. 1, calculated to include the currents from the different pathways in a double Vaseline-gap experiment; $\bar{V}$ = −48.1 mV, k = 6.1 mV, and q_{max}/c_m = 29.7 nC/μF. Same fiber as used for Figs. 1–3. First and last values: time after saponin treatment, 114–140 min; holding current, −50 and −52 nA; C_{app}, 0.01155–0.01152 μF; r_i, 2.28–2.25 MΩ/cm; c_m, 0.155–0.154 μF/cm; concentration of phenol red at the optical site, 1.384–1.509 mM; pH_R, 6.863–6.874; temperature, 14°C. The value of $[Ca_{SR}]_R$ varied between 1.0 and 6.6 μM. Additional information is given in the legend of Fig. 1.

In the experiment shown in Fig. 5 *A*, the individual values of $[Ca_{SR}]_R$ varied between 1.0 and 6.6 μM. Because it is possible that even such small amounts of SR Ca may have played a role in the production of I_γ humps, an attempt was made to reduce $[Ca_{SR}]_R$ to an even smaller value. Fig. 6 *A* shows the results of an experiment carried out on another fiber after the SR had been depleted of Ca. The traces show, from top to bottom, V_1, I_{cm}, and $\Delta[Ca_T]$ measured during two successive 600-ms pulses to −45 mV that were separated by a 500 ms period of repolarization to −90 mV.

The $\Delta[Ca_T]$ trace in Fig. 6 *A* has been heavily filtered by a 0.02 kHz digital Gaussian filter (Colquhoun and Sigworth, 1983) to reduce noise. It shows that the first pulse (labeled 1) depleted the SR of its readily releasable Ca, ~2 μM (referred to myoplasmic solution). Consequently, the value of $[Ca_{SR}]_R$ was essentially zero just before the second pulse (labeled 2), which elicited no additional discernible change in $\Delta[Ca_T]$. In spite of these measures to reduce $[Ca_{SR}]_R$, the I_{cm} trace shows prominent I_γ humps during both pulses.

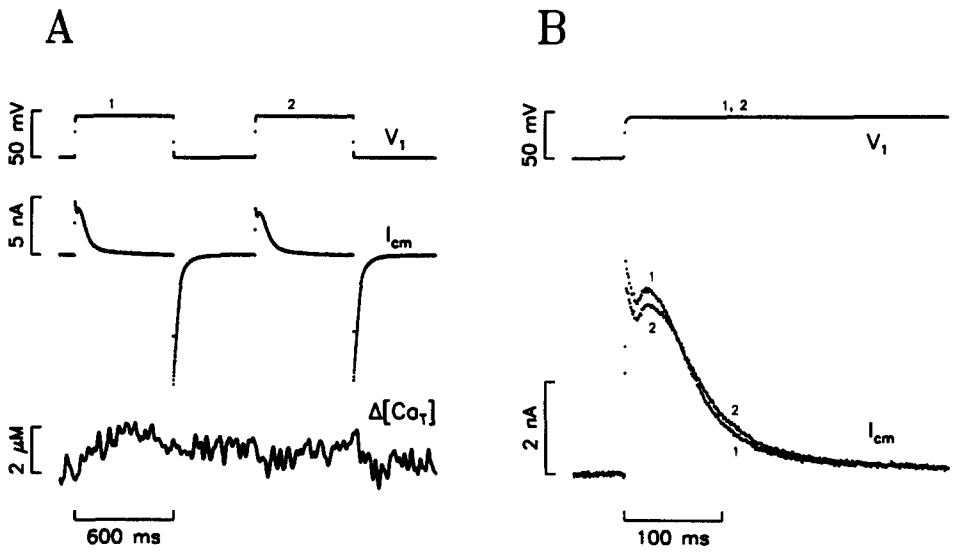

FIGURE 6. I_{cm} during two successive depolarizations to −45 mV in a Ca-depleted fiber. (*A*) The traces show, from top to bottom, V_1, I_{cm}, and $\Delta[Ca_T]$. The $\Delta[Ca_T]$ trace has been filtered by a 0.02 kHz digital Gaussian filter. (*B*) The top and bottom superimposed traces show, respectively, the initial segments of the ON V_1 and I_{cm} traces associated with the first (labeled 1) and second (labeled 2) pulses in *A*; the second pulse traces have been shifted −1,100 ms, to align the onset of the second pulse with that of the first pulse. Fiber reference, O31911; time after saponin treatment, 122 min; sarcomere length, 3.5 μm; fiber diameter, 151 μm; holding current, −44 nA; C_{app}, 0.02226 μF; r_i, 1.57 MΩ/cm; c_m, 0.307 μF/cm; concentration of phenol red at the optical site, 1.549 mM; pH_R, 6.921; temperature, 14°C; interval of time between data points, 0.96 ms.

Fig. 6 *B* shows segments of the traces in Fig. 6 *A* plotted on an expanded time scale. The top and bottom superimposed traces show, respectively, the initial part of the ON segments of the V_1 and I_{cm} traces during the first and second pulses. The I_β and I_γ peaks in the I_{cm} trace during pulse 1 are slightly larger than those during pulse 2. The two traces intersect at 50–60 ms and thereafter trace 2 is slightly above trace 1. Apart from these small differences, which were observed consistently in experiments of this type, the two I_{cm} traces are otherwise similar. In particular, they both show prominent I_γ humps. The two values of ON Q_{cm} are similar, 17.11 nC/μF during pulse 1 and 17.32 nC/μF during pulse 2. The two values of OFF Q_{cm} are also similar, −17.94 nC/μF after pulse 1 and −18.12 nC/μF after pulse 2. The traces of OFF I_{cm} after the two pulses were essentially identical (not shown).

The general conclusion of this section is that prominent I_γ humps can be elicited in the absence of SR Ca release.

After SR Ca Depletion, the Q_{cm} vs V Relation Is Steeply Voltage Dependent

Fig. 5 *B* shows the values of Q_{cm} plotted as a function of V_1, from the experiment in Fig. 5 *A*. Since the ON I_{cm} traces in Fig. 5 *A* have small amplitudes and prolonged time courses during small depolarizations, the estimates of ON Q_{cm} can be very sen-

sitive to the correction for ionic current. For this reason, the values of Q_{cm} in Fig. 5 B were taken from the values of OFF Q_{cm}. The curve shows a least-squares fit of a single Boltzmann function, Eq. 1, calculated to include the currents from the different pathways in a double Vaseline-gap experiment, as described by Hui and Chandler (1990). These gap corrections produce a foot in the curve at potentials <-60 mV and a slight negative slope at potentials >-20 mV. The best fit parameters are $\overline{V} = -48.1$ mV, $k = 6.1$ mV, and $q_{max}/c_m = 29.7$ nC/μF.

Table II gives values of the Boltzmann parameters obtained from nine fibers after SR Ca depletion. Column 1 gives the fiber references; these are the same as those in Table I except for the omission of fiber 918911 from which Q_{cm} vs V data were not obtained. Column 2 gives the times after saponin treatment, column 3 gives the duration of the pulses used to measure Q_{cm}, and column 4 gives the range of values of $[Ca_{SR}]_R$. Columns 5–7 give, respectively, the values of $\overline{V}$, k, and q_{max}/c_m. On average, $\overline{V} = -48.3$ mV, $k = 7.2$ mV, and $q_{max}/c_m = 33.5$ nC/μF. The value of k is small, indicating that Q_{cm} was steeply voltage dependent, and similar to the values observed in intact fibers that had not been Ca depleted; Table VII in Hui and Chandler (1990) gives the Boltzman parameters obtained in intact fibers by several laboratories.

Hui and Chandler (1990) measured the Q_{cm} vs V relation in cut fibers equilibrated with an internal solution that was similar to the one used here except for the presence of 0.4 mM total Ca in their solutions. Their external solution contained

TABLE II

Parameters Associated with Charge Movement after SR Ca Depletion

(1)	(2)	(3)	(4)	(5)	(6)	(7)
Fiber	Time after saponin	Pulse duration	$[Ca_{SR}]_R$	$\overline{V}$	k	q_{max}/c_m
	min	*ms*	*μM*	*mV*	*mV*	*nC/μF*
N28901	114–140	200	1.0 to 6.6	−48.1	6.1	29.7
D17902	98–126	400	0.2 to 18.5	−46.8	8.5	27.6
416911	114–132	800	1.1 to 6.6	−44.3	7.5	34.1
O17911	148–183	600	−1.5 to 3.9	−48.6	7.1	40.4
O31911	124–152	800	1.1 to 3.9	−50.3	7.8	32.7
N05911	131–152	100-600	3.8 to 11.6	−50.3	6.4	31.9
N06911	128–147	200-600	3.1 to 12.6	−51.2	7.1	29.8
N07911	128–147	200-600	4.2 to 11.9	−47.2	6.5	35.5
N08911	135–155	200-600	5.4 to 10.8	−48.0	7.4	39.6
Mean				−48.3	7.2	33.5
SEM				0.7	0.3	1.5

Column 1 gives the fiber references. Column 2 gives the initial and final values of the time after saponin treatment. Column 3 gives the duration of the pulses used for the measurement of Q_{cm}; when a range of values is given, the shortest duration pulses were used with the most positive depolarizations. Column 4 gives the range of values of $[Ca_{SR}]_R$. Columns 5–7 give the values of $\overline{V}$, k, and q_{max}/c_m that were obtained from least-squares fits, with gap corrections, of a single Boltzmann function to Q_{cm} vs voltage data (as illustrated in Fig. 5 *B*). Sarcomere length, 3.3–3.5 μm; fiber diameter, 89–159 μm; holding current, −30 to −58 nA; r_i, 1.58–2.52 MΩ/cm; c_m, 0.154–0.307 μF/cm; concentration of phenol red at the optical site, 1.069–2.234 mM; pH_R, 6.704–6.921 μM; temperature, 13–16°C.

tetraethylammonium chloride and 1.8 mM Ca. Although SR Ca release was not measured, $[Ca_{SR}]_R$ was probably >100 μM because of the presence of Ca in the internal and external solutions. A least-squares fitting procedure similar to that used in Table II gave, on average, $\overline{V}$ = −51.2 mV (SEM, 1.1 mV), k = 7.2 mV (SEM, 0.4 mV), and q_{max}/c_m = 22.9 nC/μF (SEM, 1.4 nC/μF) (Table II in Hui and Chandler, 1990). Their mean values of $\overline{V}$ and k are not significantly different from those in Table II. In contrast, their mean value of q_{max}/c_m is significantly less than that in Table II. The reason for this difference is not known but may be related to the use of different anions in the external solutions: Hui and Chandler (1990) used chloride whereas we used gluconate.

In the experiments of Hui and Chandler (1990), the Q_{cm} vs V relation was clearly asymmetrical and poorly fitted by a single Boltzmann function. A significantly better fit was obtained with two Boltzmann functions, which were tentatively identified with the Q_β and Q_γ components of charge movement. The values of q_{max}/c_m were similar for the two components, 10.6 nC/μF for Q_β and 13.2 nC/μF for Q_γ. The values of $\overline{V}$ and k were different, however; $\overline{V}$ = −33.0 mV for Q_β and −56.5 mV for Q_γ and k = 11.0 mV for Q_β and 2.9 mV for Q_γ. The combination of different values of $\overline{V}$ and of k accounts for the asymmetry in their Q_{cm} vs V relation.

In the experiments reported here, a single Boltzmann function provides a good fit to the Q_{cm} vs V data, as illustrated in Fig. 5 *B*. Fits were also carried out with two Boltzmann functions (not shown) so that the statistical test described on pages 276–278 in Hui and Chandler (1990) could be used to determine whether the fit with two Boltzmann functions was significantly better than the fit with one Boltzmann function. Significant improvement occurred in only two out of nine fibers. In each of these two fibers, however, the improvement was spurious because one of the two values of q_{max}/c_m was negative.

A possible explanation of the good fits provided by a single Boltzmann function in our experiments is that, because of the use of gluconate in the external solution (Chen and Hui, 1991), Q_γ accounted for most of the charge with a mean value of 7.2 mV, instead of 2.9 mV, for k. Another possibility is that the values of $\overline{V}$ for Q_β and Q_γ might have been similar, in which case a good fit to the data would be expected to be provided by a single Boltzmann function with a value of k that lies between those for Q_β and Q_γ. Additional information is required to decide between either of these and other possibilities.

The results in Fig. 5, *A* and *B*, Fig. 6, and Table II show that the two most distinctive characteristics of Q_γ charge—the presence of a hump component in the ON I_{cm} and a steeply voltage dependent Q_{cm} vs V relation—are present after SR Ca depletion. In these experiments, the main effect of small amounts of SR Ca, no more than a few hundred micromolar, appears to be on the ON kinetics of I_γ.

After SR Ca Depletion, the Time Course of OFF I_{cm} Varies with the Amplitude of the Pulse

Fig. 7 A shows values of the half-width of OFF I_{cm} plotted as a function of voltage during the ON pulse, from the experiment illustrated in Fig. 5 A; for this purpose, half-width is defined as the interval from the time to half-peak on the rising phase of I_{cm} until the time to half-peak on the falling phase of I_{cm}. For voltages between

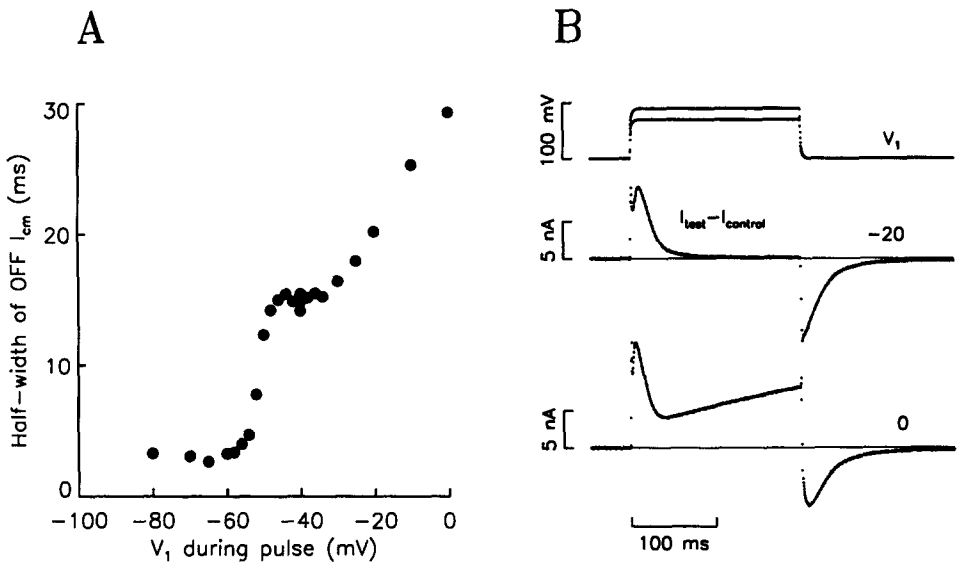

FIGURE 7. Effect of pulse potential on OFF I_{cm} in a Ca-depleted fiber, from the experiment in Fig. 5. (*A*) The half-width of OFF I_{cm} is plotted as a function of the pulse potential. (*B*) $I_{test} - I_{control}$ during pulses to −20 and 0 mV, with V_1 indicated (in millivolts). Thin horizontal lines show the prestimulus baselines. See text and legend of Fig. 5 for additional information.

−80 and −60 mV, the value of the half-width was relatively constant at ~3 ms. From −56 to −46 mV, it increased from ~4 to ~15 ms and then remained relatively constant at ~15 ms from −46 to −34 mV. From −30 to 0 mV, it increased about twofold, from 16 to 29 ms.

In the experiment in Fig. 7 *A*, little, if any, ionic current developed during the pulses to voltages between −80 and −20 mV (Fig. 5 *A*). Consequently, the OFF I_{cm} traces are not expected to be contaminated by ionic current, such as might happen if a conductance that had been activated during the depolarization allowed ionic current to flow during the repolarization. When the potential was more positive than −20 mV, however, a small outward current developed during the pulse and the OFF kinetics of I_{cm} became slower.

The effect of pulses to −20 and 0 mV on OFF I_{cm} is illustrated in Fig. 7 *B*. The top superimposed pair of traces shows V_1 associated with pulses to −20 and 0 mV. The next trace shows $I_{test} - I_{control}$ for −20 mV. The steady level during the pulse was constant and close to the prestimulus baseline (*thin horizontal line*), indicating that the ionic conductance between −110 and −20 mV was essentially constant and did not change during the pulse. After repolarization from − 20 to −90 mV, the OFF I_{cm} rapidly decreased, reached a minimum value of −11.1 nA at ~2 ms, and then decayed to near the prestimulus baseline. The I_{cm} trace that was obtained from this $I_{test} - I_{control}$ trace is shown at the bottom of Fig. 5 *A*.

The bottom trace in Fig. 7 *B* shows $I_{test} - I_{control}$ for a pulse to 0 mV. At this potential, a small outward current developed during the pulse, presumably due to an increase in ionic conductance. After repolarization, the time course of OFF I_{cm} was

qualitatively different from that after the pulse to −20 mV: the tail current developed more slowly and reached a smaller (in absolute magnitude) minimal value, −7.7 nA, after a longer period of time, 10 ms after repolarization. Since a small ionic conductance developed during the pulse to 0 mV, it is possible that the estimated OFF I_{cm} contains a contribution from ionic current that flowed through this conductance. Although it is difficult to assess the magnitude of this contribution without knowledge of the reversal potential of the current and possibly the time course of its decay during repolarization, it might be small if the reversal potential were close to the holding potential, −90 mV. This may have been the case since the total amount of OFF Q_{cm} after the pulse to 0 mV was similar to that after the pulse to −20 mV (Fig. 5 *B*). Another finding supports the idea that ionic contamination made little contribution to the slow development of the OFF I_{cm} tail after the pulse to 0 mV: similar tails with slow kinetics were sometimes observed after pulses to less positive potentials where changes in conductance were absent (Fig. 8 *A*).

The general features of the results illustrated in Fig. 7 were found in all nine experiments reported in Table II. As the pulse potential was increased from −80 to −60 mV, the half- width of OFF I_{cm} showed a small increase in two experiments, was relatively constant in five experiments (one of which is illustrated in Fig. 7 *A*), and showed a small decrease in two experiments. As the pulse potential was made more positive than ~−60 mV, all of the fibers showed an increase in half-width followed by a plateau, although the characteristics of the sharp increase (from −52 to −46 mV in Fig. 7 *A*) and the plateau (from −46 to −34 mV in Fig. 7 *A*) were somewhat variable. In all experiments, the development of the OFF I_{cm} tail became progressively delayed from −30 to 0 mV and the half-width progressively increased.

Hui and Chandler (1991) also observed a sigmoid relation between the half-width of OFF I_{cm} and voltage, similar to that illustrated in Fig. 7 *A*. The main difference between their results and ours was observed at voltages more positive than −30 mV: in their experiments (see their Fig. 8), the half- width decreased with increasing potential whereas, in our experiments, it increased. This difference is probably not due to SR Ca release in their experiments, as described in the preceding section, since release has little effect on the half-width of OFF I_{cm} after a long lasting depolarization (see Fig. 2). Rather, it seems likely that the difference may have been due to a relatively greater amount of I_β in their experiments because chloride rather than gluconate was used in the external solution.

After SR Ca Depletion, the Time Course of OFF I_{cm} Varies with the Duration of the Pulse

Fig. 8 *A* shows six superimposed traces of voltage (*top*) and I_{cm} (*bottom*) associated with different duration pulses to −45 mV, in a fiber with $[Ca_{SR}]_R \leq 4$ μM. In this experiment, the I_{cm} traces show little, if any, I_β component so that the I_γ hump is particularly prominent. After the two briefest pulses, of duration 10 and 20 ms, OFF I_{cm} rapidly reached a peak (negative) value and then rapidly decayed towards zero. After the longer pulses, I_{cm} did not reach a peak value until 5–10 ms after repolarization and the duration of its time course was prolonged.

Fig. 8 *B* shows the negative values of OFF Q_{cm} plotted as a function of ON Q_{cm}. The straight line shows a least-square fit to the data, constrained to intersect the or-

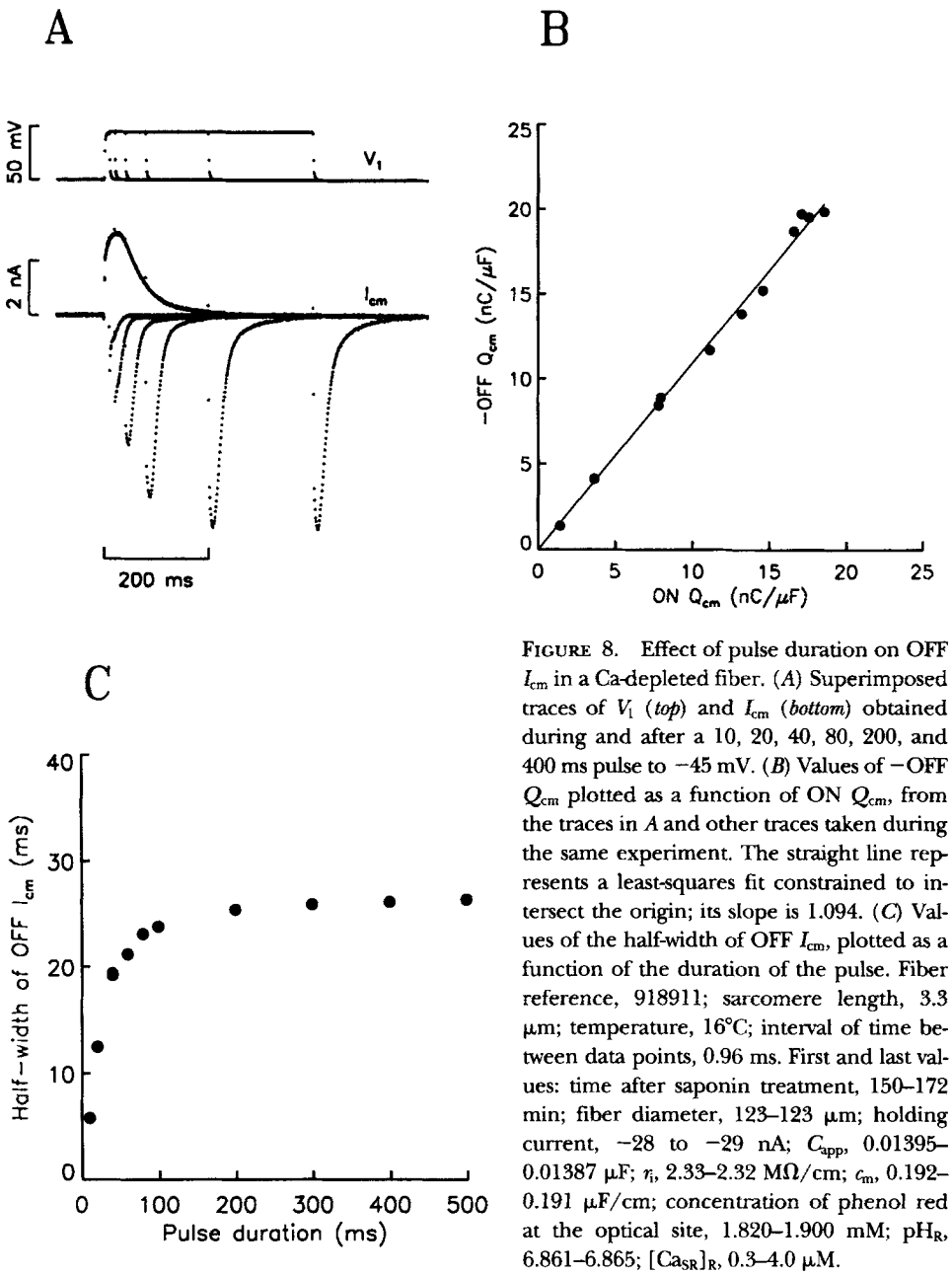

FIGURE 8. Effect of pulse duration on OFF I_{cm} in a Ca-depleted fiber. (*A*) Superimposed traces of V_1 (*top*) and I_{cm} (*bottom*) obtained during and after a 10, 20, 40, 80, 200, and 400 ms pulse to −45 mV. (*B*) Values of −OFF Q_{cm} plotted as a function of ON Q_{cm}, from the traces in *A* and other traces taken during the same experiment. The straight line represents a least-squares fit constrained to intersect the origin; its slope is 1.094. (*C*) Values of the half-width of OFF I_{cm}, plotted as a function of the duration of the pulse. Fiber reference, 918911; sarcomere length, 3.3 μm; temperature, 16°C; interval of time between data points, 0.96 ms. First and last values: time after saponin treatment, 150–172 min; fiber diameter, 123–123 μm; holding current, −28 to −29 nA; C_{app}, 0.01395–0.01387 μF; r_i, 2.33–2.32 MΩ/cm; c_m, 0.192–0.191 μF/cm; concentration of phenol red at the optical site, 1.820–1.900 mM; pH_R, 6.861–6.865; $[Ca_{SR}]_R$, 0.3–4.0 μM.

igin. Although its slope, 1.094, is significantly different from unity according to the test described in the Methods section, it seems likely that the difference is due to a small inaccuracy in the determination of the ionic component of $I_{test} - I_{control}$ that was used to estimate I_{cm} rather than to a genuine inequality of ON-OFF charge (see

above discussion of Table I). Thus, this experiment provides good evidence that the ON and OFF traces of I_{cm} in Fig. 8 *A* represent currents from intramembranous charge movement.

Fig. 8 *C* shows values of the half-width of OFF I_{cm}, plotted as a function of pulse duration. The data progressively increase from a value of ~6 ms after the shortest pulse, of duration 10 ms, to a plateau value of ~26 ms for pulse durations ≥300 ms. As shown in Fig. 8 *A*, these changes in half-width were accompanied by little, if any, change in ionic conductance during the depolarizing pulse. The relation between the half-width of OFF I_{cm} and pulse duration in Fig. 8 *C* is similar to that observed by Hui and Chandler (1991) (see traces in their Fig. 10).

The general conclusion of this and the preceding section is that the time course of OFF I_{cm} varies with the amplitude and duration of the ON pulse, even after the SR has been depleted of almost all of its readily releasable Ca. With pulse potentials ≤ −20 mV, little, if any, change in ionic conductance occurred during the pulse, making it unlikely that the OFF I_{cm} was contaminated by ionic current. The characteristics of the variation of the half-width of OFF I_{cm} with pulse potential are consistent with the idea that, as charge moves progressively from its resting to its final state during a depolarization, the kinetics of its return after repolarization become progressively slower. This idea is incorporated into the theoretical model of charge movement that is described in the Discussion.

The ON Kinetics of I_{cm} Can Be Described Empirically in Terms of k_{app}

The time course of ON I_{cm} can be described empirically in terms of k_{app}, the apparent rate constant for charge movement, as illustrated in Fig. 9. The top two traces show the ON V_1 and I_{cm} traces from Fig. 1. The third trace shows Q_{cm}, the running integral of I_{cm}, divided by C_{app}, the apparent capacitance of the fiber, 0.01158 μF (see Eq. 2 in Hui and Chandler, 1990). The horizontal line shows the mean value of Q_{cm} during the final 7.2 ms of the pulse. Its value, 20.3 nC/μF, will be denoted by $Q_{cm}(\infty)$. At any moment in time, $Q_{cm}(\infty) - Q_{cm}$ gives the amount of charge that remains to be moved. The bottom trace shows k_{app}. It was obtained by dividing I_{cm}/C_{app} by $Q_{cm}(\infty) - Q_{cm}$ and converting to units of %/ms. Thus, at any instant, the value of I_{cm} is proportional to k_{app} times $Q_{cm}(\infty) - Q_{cm}$.

The k_{app} trace in Fig. 9 rapidly increased after depolarization and, after ~1 ms, reached an early peak value of ~3%/ms. After a slight dip, the trace then increased to a larger peak value of 6.4%/ms. Thereafter, the trace decreased somewhat and became progressively noisier as the value of $Q_{cm}(\infty) - Q_{cm}$ (the denominator in the expression for k_{app}) became smaller. A comparison of the time courses of the I_{cm} and k_{app} traces shows that the I_γ hump in the I_{cm} trace is associated with a hump in the k_{app} trace.

The Effect of $[Ca_{SR}]_R$ on the Time Course of k_{app}

Fig. 10 shows k_{app} and the rate of SR Ca release with different values of $[Ca_{SR}]_R$. These traces were obtained from those in Fig. 2 after they had been filtered with a 0.05 kHz digital Gaussian filter (Colquhoun and Sigworth, 1983) to reduce noise, especially in $d\Delta[Ca_T]/dt$.

The first set of four traces shows k_{app}, obtained from the traces of I_{cm} in the man-

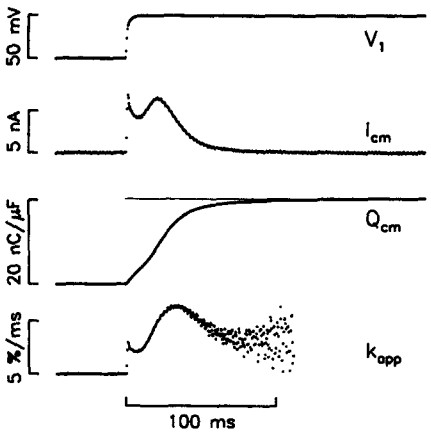

FIGURE 9. Determination of k_{app} for ON I_{cm}. The top two traces show V_1 and ON I_{cm} from Fig. 1. The third trace shows Q_{cm}, with a thin horizontal line drawn through the mean value of the last 7.2 ms, 20.3 nC/μF, denoted by $Q_{cm}(\infty)$ in the text. The bottom trace shows k_{app}. Additional information is given in the text.

ner illustrated in Fig. 9. Trace 2 is the same as the bottom trace in Fig. 9 except for the use of the Gaussian filter, which smoothed the trace and reduced its peak amplitude by ~1%. In Fig. 10, the early component of k_{app} was similar for the four traces whereas the hump component became somewhat more pronounced from 1 to 2 and then became smaller in 3 and 4. This shows that the main effect of $[Ca_{SR}]_R$ on k_{app} is on the hump component. After ~80 ms, traces 2–4 were similar to each other and had slightly larger values than trace 1. The smaller amplitude of trace 1 is probably due to an inhibitory effect of SR Ca on I_{cm} that becomes apparent once $[Ca_{SR}]_R$ exceeds a few hundred micromolar (Pape, Jong, and Chandler, 1992; 1996). This inhibitory effect probably also accounts for the observation that trace 1 lies below trace 2 after 25–30 ms and has a slightly smaller peak value.

The second set of four traces in Fig. 10 shows $[k_{app}/k_{app,0} - 1]$; $k_{app,0}$ denotes k_{app} from trace 4 in which $[Ca_{SR}]_R \cong 0$ μM. The value of $[k_{app}/k_{app,0} - 1]$ provides an estimate of the effect of SR Ca on k_{app}; a value of zero indicates no effect (that is, $k_{app} = k_{app,0}$), a positive value indicates an increase in k_{app}, and a negative value indicates a decrease. Traces 1 and 2 have peak values of $[k_{app}/k_{app,0} - 1]$ that are >1, which

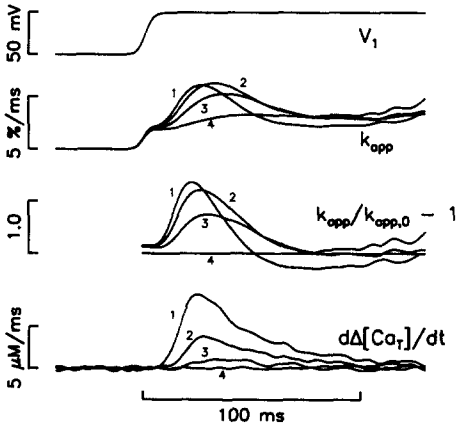

FIGURE 10. The effect of SR Ca on the time course of k_{app}. The top trace shows V_1. The next sets of superimposed traces show, from top to bottom, k_{app}, $[k_{app}/k_{app,0} - 1]$, and $d\Delta[Ca_T]/dt$. These were obtained from the traces in Fig. 2 after using a 0.05 kHz digital Gaussian filter to reduce noise, as described in the text.

means that the value of k_{app} had been more than doubled by the effect(s) of Ca inside the SR. The negative segment of trace 1 at times >50 ms indicates an overall inhibitory effect on k_{app}, as mentioned in the preceding paragraph.

The bottom set of traces in Fig. 10 shows $d\Delta[Ca_T]/dt$. The time course of each of the $d\Delta[Ca_T]/dt$ traces is roughly similar to that of the corresponding $[k_{app}/k_{app,0} - 1]$ trace. This similarity is of interest because, in these experiments in which only a small amount of Ca is released in the presence of EGTA and phenol red, the changes in myoplasmic free [Ca] that accompany SR Ca release are expected to be confined to within a few hundred nanometers of the release sites and to have a time course that is approximately the same as that of $d\Delta[Ca_T]/dt$, with a proportionality constant that varies inversely with distance from the release sites (Pape et al., 1995). Thus, the similarity of the corresponding $[k_{app}/k_{app,0} - 1]$ and $d\Delta[Ca_T]/dt$ traces is consistent with the idea that an increase in myoplasmic free [Ca] somewhere near the release sites is able to increase the value of k_{app} (see last section of Discussion).

The Effect of SR Ca on the Peak Value of $[k_{app}/k_{app,0} - 1]$

Fig. 11 *A* shows the peak value of $[k_{app}/k_{app,0} - 1]$ plotted as a function of $[Ca_{SR}]_R$. Since the main effect of SR Ca on k_{app} may be due to its effect on the rate of SR Ca release, Fig. 11 *B* shows the same values of $[k_{app}/k_{app,0} - 1]$ plotted as a function of peak $d\Delta[Ca_T]/dt$. A plot of similar appearance would have been obtained if the value of $[k_{app}/k_{app,0} - 1]$ had been plotted against the peak increase in free [Ca] at

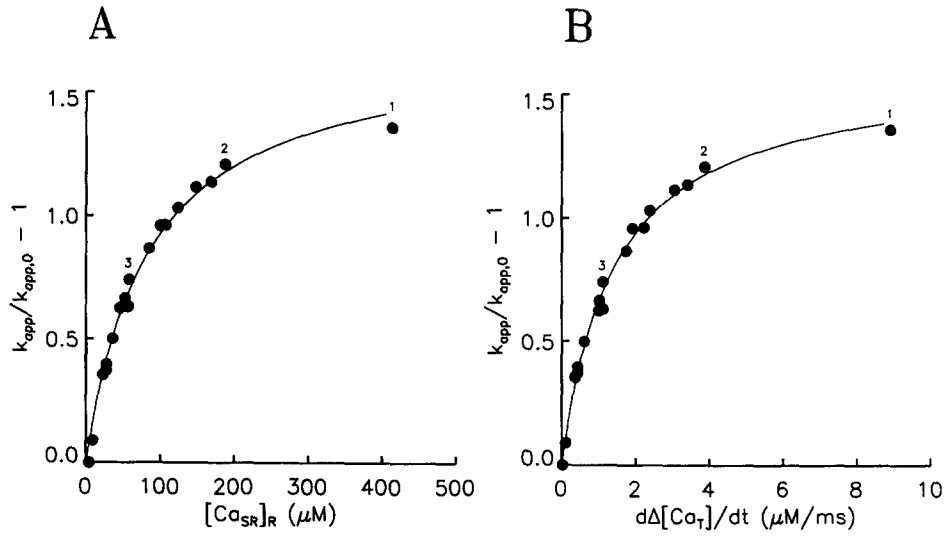

FIGURE 11. The effect of SR Ca on $[k_{app}/k_{app,0} - 1]$, from the experiment illustrated in Fig. 10. The peak values of $[k_{app}/k_{app,0} - 1]$ are plotted as a function of $[Ca_{SR}]_R$ in *A* and of the peak value of $d\Delta[Ca_T]/dt$ in *B*. The curves were obtained from least-squares fits of Eq. 5, with $[k_{app}/k_{app,0} - 1]_{max}$ = 1.71 and $[Ca_{SR}]_{R,1/2}$ = 85 μM in *A* and $[k_{app}/k_{app,0} - 1]_{max}$ = 1.61 and $d\Delta[Ca_T]/dt_{1/2}$ = 1.43 μM/ms in *B*.

a particular location in the myoplasm near the release sites, since such increases are expected to be proportional to $d\Delta[Ca_T]/dt$ (preceding paragraph). In Fig. 11 *A* (or Fig. 11 *B*), $[k_{app}/k_{app,0} - 1]$ increases steeply with $[Ca_{SR}]_R$ (or peak $d\Delta[Ca_T]/dt$) near the origin and tends towards a plateau value at large values of $[Ca_{SR}]_R$ (or peak $d\Delta[Ca_T]/dt$).

The curves in Figs. 11, *A* and *B*, represent least-squares fits of the equation for 1:1 binding,

$$[k_{app}/k_{app,0} - 1] = [k_{app}/k_{app,0} - 1]_{max} \cdot \frac{x}{x + x_{1/2}} \quad (5)$$

$[k_{app}/k_{app,0} - 1]_{max}$ represents the maximal value of $[k_{app}/k_{app,0} - 1]$, x represents $[Ca_{SR}]_R$ in *A* and peak $d\Delta[Ca_T]/dt$ in *B*, and $x_{1/2}$ represents the value of x for half-maximal response. Eq. 5 was used empirically to provide estimates of $[k_{app}/k_{app,0} - 1]_{max}$ (1.71 in *A* and 1.61 in *B*), $[Ca_{SR}]_{R,1/2}$ (85 μM in *A*), and $d\Delta[Ca_T]/dt_{1/2}$ (1.4 μM/ms in *B*).

In the ten fibers used for Table I, traces of $[k_{app}/k_{app,0} - 1]$ were obtained at different times during SR Ca depletion and were analyzed as illustrated in Fig. 11. Table III gives some of the information obtained from these analyses. Column 1 gives the fiber references and column 2 gives the values of the voltages of the pulses. The table is arranged in sections according to pulse potential, −50 mV (*A*), −45 mV (*B*), −40 mV (*C*), and −30 mV (*D*).

In the five fibers listed in Table III *D*, traces of $[k_{app}/k_{app,0} - 1]$ were obtained both at −30 mV and at −50 or −45 mV by switching the pulse amplitude between successive stimulations. The duration of the pulses was long, 600–750 ms, and, at −30 mV, the ON $I_{test} - I_{control}$ traces had a small slope after the charge movement current had been completed. For this reason, no attempt was made to assess ON-OFF charge equality as was done for pulse potentials between −50 and −40 mV (Table I). Fortunately, the early portions of the $[k_{app}/k_{app,0} - 1]$ traces, up to the time of peak, were relatively insensitive to the exact values of $Q_{cm}(\infty)$ that were used to estimate k_{app} and $k_{app,0}$, so that reliable fits of Eq. 5 could be made.

Columns 3–6 of Table III give the values of the parameters obtained from fits of Eq. 5 to the peak values of $[k_{app}/k_{app,0} - 1]$. In each column, at the end of each section, letters in parentheses reference the other sections that have significantly different mean values. Thus, the listing (*B, D*) in column 3 of section *A* means that the mean value of 6.32 in A is significantly different from 1.63 in *B* and 0.31 in *D* but is not significantly different from 1.47 in *C*.

The values of the parameters in Table III show three general trends. Firstly, the values of $[k_{app}/k_{app,0} - 1]_{max}$ (columns 3 and 5) decrease as the pulse potential is increased from −50 to −30 mV. Secondly, the values of $[Ca_{SR}]_{R,1/2}$ (column 4) show a tendency to decrease with increasing pulse potential, although only the changes from −50 to −45, −40, and −30 mV are significant. Thirdly, the values of $d\Delta[Ca_T]/dt_{1/2}$ (column 6) are not significantly different from each other. Their independence of pulse potential is consistent with the idea that the main effect of SR Ca on k_{app} is caused by $d\Delta[Ca_T]/dt$, perhaps through a change in myoplasmic free [Ca] near the release sites (see preceding section). Some of the implications of these results are considered in the Discussion.

TABLE III

Effect of $[Ca_{SR}]_R$ or $d\Delta[Ca_T]/dt$ on $[k_{app}/k_{app,0} - 1]$

(1)	(2)	(3)	(4)	(5)	(6)
Fiber	V_1	$[k_{app}/k_{app,0}-1]_{max}$	$[Ca_{SR}]_{R,1/2}$	$[k_{app}/k_{app,0} - 1]_{max}$	$d\Delta[Ca_T]/dt_{1/2}$
	mV		*μM*		*μM/ms*
A					
N07911	−50	4.27	352	3.17	1.14
N08911	−50	8.36	505	4.62	1.73
Mean	−50	6.32	429	3.90	1.44
SEM		2.05	77	0.73	0.30
		(*B, D*)	(*B, C, D*)	(*B, D*)	
B					
416911	−45	2.16	222	1.74	1.06
918911	−45	1.61	129	1.41	1.05
O17911	−45	1.22	71	1.08	0.44
O31911	−45	1.17	122	1.07	1.08
N05911	−45	2.23	310	1.78	2.54
N06911	−45	1.38	178	1.15	1.31
Mean	−45	1.63	172	1.37	1.25
SEM		0.19	35	0.13	0.28
		(*A, D*)	(*A*)	(*A, D*)	
C					
N28901	−40	1.71	85	1.61	1.43
D17902	−40	1.22	81	1.15	0.88
Mean	−40	1.47	83	1.38	1.16
SEM		0.25	2	0.23	0.28
		(*D*)	(*A*)	(*D*)	
D					
918911	−30	0.38	158	0.34	1.99
O17911	−30	0.26	71	0.25	0.75
O31911	−30	0.23	114	0.22	1.50
N06911	−30	0.20	126	0.18	1.38
N08911	−30	0.49	125	0.38	1.33
Mean	−30	0.31	119	0.27	1.39
SEM		0.05	14	0.04	0.20
		(*A, B, C*)	(*A*)	(*A, B, C*)	

Column 1 gives the fiber references and column 2 gives the voltage during the pulse. Columns 3 and 4 give the values of $[k_{app}/k_{app,0} - 1]_{max}$ and $[Ca_{SR}]_{R,1/2}$, respectively, that were obtained by fitting Eq. 5 to $[k_{app}/k_{app,0} - 1]$ plotted against $[Ca_{SR}]_R$, as shown in Fig. 11 *A*. Columns 5 and 6 give the values of $[k_{app}/k_{app,0} - 1]_{max}$ and $d\Delta[Ca_T]/dt_{1/2}$, respectively, obtained from $[k_{app}/k_{app,0} - 1]$ plotted against peak $d\Delta[Ca_T]/dt$, as shown in Fig. 11 *B*. Sections *A*, *B*, *C*, and *D* give values associated with $V_1 = -50$, -45, -40, and -30 mV, respectively. In columns 3–6, letters in parentheses at the end of each section reference the other sections that have mean values that are significantly different. Additional information is given in Table I.

DISCUSSION

This article describes measurements of SR Ca release and intramembranous charge movement in fibers in which the value of $[Ca_{SR}]_R$ was reduced from several hundred micromolar to <10 μM by repeated depolarizations after equilibration with Ca-free internal and external solutions. During the period when the value of $[Ca_{SR}]_R$ was decreasing, changes were observed in the time course of ON I_{cm}, especially that of the I_γ component. After essentially all of the readily releasable Ca had

been removed from the SR, prominent I_γ humps and steep Q_{cm} vs V relations were consistently observed (Fig. 5 and Table II). These observations confirm those of Csernoch et al. (1991), García et al. (1991), Szucs et al. (1991), and Pizarro et al. (1991), who first showed that I_{cm} could be affected by SR Ca content or release or some related event. On the other hand, the observations do not support the proposal of these authors that I_γ represents a movement of Q_β charge that is caused by SR Ca release (see Introduction). Because charge movement currents with the properties of I_γ can be elicited without any readily releasable Ca inside the SR, our results suggest that Q_β and Q_γ represent either two distinct species of charge (Adrian and Huang, 1984; Huang, 1986, 1994*b*; Huang and Peachy, 1989; Hui and Chandler, 1991) or two transitions with different properties of a single species of charge (for example, see Melzer et al., 1986).

Comparison of the Properties of Charge Movement in Ca-depleted Fibers with Predictions from Two Published Models

Since our experiments on Ca-depleted fibers provide information about the fundamental properties of intramembranous charge movement, unaltered by any effects of SR Ca, it is clearly of interest to compare our results with theoretical models of charge movement such as those proposed by Huang (1984) and by Ríos et al. (1993).

In the model proposed by Huang (1984), Q_γ charge is assumed to occupy one of two states, resting and activating. Huang used the variable q to represent the fractional amount of charge in the activating state and assumed that dq/dt, which is proportional to I_γ, obeys

$$dq/dt = \alpha(1 - q) - \beta q. \tag{6}$$

α and β represent, respectively, the forward and backward rate constants for transitions between the resting and activating states. As is well known, if the values of α and β are functions of only V, the time course of I_γ during a step depolarization is exponential and does not show humps.

To generate I_γ humps, Huang (1984) proposed that α and β depend on q, as well as on V, according to

$$\alpha = \alpha_0(V)\,(1 + \zeta q), \tag{7}$$

$$\beta = \beta_0(V)\,(1 + \zeta q). \tag{8}$$

$\alpha_0(V)$ and $\beta_0(V)$ are the rate constants associated with $q = 0$, and ζ is a positive constant. Eq. 6–8 are similar to Eqs. 1–3 in Huang (1984). After a step change in potential from its resting level to V, the values of q, α, and β progressively increase from their initial values (approximately zero, $\alpha_0(V)$, and $\beta_0(V)$, respectively) towards new larger steady state values. With suitable choices of $\alpha_0(V)$ and $\beta_0(V)$, and ζ, pronounced I_γ humps can be demonstrated (Fig. 8 in Huang, 1984).

Although this model is able to account for prominent ON I_γ humps, it does not account for the experimental finding that the OFF half-width progressively increases with either the potential or duration of a pulse. As the potential or duration

of a pulse is increased, the value of q that is attained at the end of the pulse is increased. This increases the value of the factor that multiplies $\alpha_0(V)$ and $\beta_0(V)$ in Eqs. 7 and 8 so that, after repolarization, the values of α and β are increased and the value of OFF half-width is decreased. Thus, according to Huang's (1984) model, the OFF half-width progressively consisting decreases with either the potential or duration of a pulse, which is exactly the opposite of the effect that is observed experimentally.

Since the publication of Huang's article, Ríos and Brum (1987) and Tanabe, Beam, Powell, and Numa (1988) have shown that the voltage sensor for the control of SR Ca release appears to consist of one or more dihydropyridine receptors (DHPR). Block, Imagawa, Campbell, and Franzini-Armstrong (1988) have observed regular arrays of tetrads (presumably consisting of DHPR's) in the membranes of the transverse tubular system. This raises the possibility that each voltage sensor consists of four charge movement particles (presumably DHPR's).

In an attempt to explain the effects of perchlorate on charge movement and SR Ca release, Ríos et al. (1993) proposed a model in which a single SR Ca channel is activated by four identical charge movement particles. The model predicts small I_γ humps that resemble those that they observed experimentally, both in the absence and presence of perchlorate. These humps, however, were considerably less pronounced than those reported here, even after Ca depletion (Figs. 5 *A*, 6, and 8). It therefore seemed important to find out whether pronounced I_γ humps could be obtained by suitable adjustment of the parameters in their model. Because their model has seven adjustable parameters, many combinations of values must be explored to determine which ones give the most pronounced I_γ humps. These calculations are described in the Appendix. They show that pronounced I_γ humps, such as those observed in Figs. 5 *A*, 6, and 8, cannot be calculated with any set of parameters that is consistent with both the steady state Q_{cm} vs V data and the small rate of Ca flux that is expected from the resting SR.

The conclusion of this section is that the models proposed by Huang (1984) and Ríos et al. (1993) fail, in major ways, to account for the properties of Q_γ charge movement. We have not attempted to modify the basic form of either model, although such modifications might produce fruitful results. Rather, we have explored other kinds of models, all based on four interacting charge movement particles as suggested by the observation of tetrads in the membranes of the transverse tubular system (Block et al., 1988). One of these models is described in the following section.

A Model of Q_γ Based on Four Interacting Charge Movement Particles

The aim of this section is to describe a simple kinetic model of Q_γ and to show that it is generally consistent with the experimental results on Ca-depleted fibers reported in this article. In the model, I_γ is assumed to arise from voltage sensors in the membranes of the transverse tubular system. Each voltage sensor is assumed to consist of four identical charge movement particles, as suggested by the work of Block et al. (1988) that is described in the preceding section. Each of the four charge movement particles is assumed to be in one of two states, resting and activating. As a result, each voltage sensor has five states, depending on whether 0, 1, 2, 3,

or 4 charge movement particles are in the activating state. Schemes of this type have been used in studies of ionic channel gating, as reviewed recently by Sigworth (1993) and Bezanilla and Stefani (1994).

Let x_n denote the fraction of voltage sensors that have n charge movement particles in the activating state ($x_0 + x_1 + x_2 + x_3 + x_4 = 1$). Let α_n and β_n denote the forward and backward rate constants for transitions between states n and $n + 1$, with $n = 0$, 1, 2, or 3. The values of α_n and β_n are assumed to depend only on V and n. Changes in the values of x_n can be described in terms of the reaction sequence

$$x_0 \underset{\beta_0}{\overset{4\alpha_0}{\rightleftharpoons}} x_1 \underset{2\beta_1}{\overset{3\alpha_1}{\rightleftharpoons}} x_2 \underset{3\beta_2}{\overset{2\alpha_2}{\rightleftharpoons}} x_3 \underset{4\beta_3}{\overset{\alpha_3}{\rightleftharpoons}} x_4 .$$

REACTION SEQUENCE I

The equilibrium distributions between states n and $n + 1$ are assumed to satisfy the Boltzmann distribution law. For $n = 0$, this condition can be written

$$\alpha_0/\beta_0 = \exp(y) , \tag{9}$$

in which

$$y = (V - \overline{V})/k . \tag{10}$$

$\overline{V}$ and k are constants.

In all of the examples described below, each value of α_n/β_n for $n = 1$, 2, or 3 is assumed to be given by a constant, voltage-independent factor times α_0/β_0, which is equal to the same factor times $\exp(y)$ (Eq. 9). In this situation, the same value of k (Eq. 10) applies to all four transitions in reaction sequence I. Consequently, each transition gives rise to the same amount of charge movement.

If all four charge movement particles in a voltage sensor are able to move independently of one other, the values of α_n and β_n would be independent of n. In this case, the relation $\alpha_n/\beta_n = \exp(y)$ would apply to all values of n (Eq. 9), the equilibrium Q_γ vs V relation would be given by the Boltzmann distribution function (Eq. 1), and I_γ would follow an exponential time course during a step change in potential.

In general, however, movements of the four particles may not occur independently. Three such cases are considered below. In the first case, the equilibrium Q_γ vs V relation obeys the Boltzmann distribution whereas, in the second and third case, it does not. In all three cases, the value of I_γ changes immediately after a step change in potential, as reported by Huang (1994*b*), and then follows a nonexponential time course.

Case 1: $\alpha_n = f^n \alpha_0$ and $\beta_n = f^n \beta_0$. As described in the preceding section, Huang (1984) proposed a scheme that, in many ways, represents an extension of reaction sequence I for the case in which the number of charge movement particles is large. The values of α and β are assumed to increase monotonically with the fraction of charge particles in the activating state, Eqs. 6–8. This increase is subject to the constraint that the value of α/β is maintained constant so that the equilibrium distribution of charge movement particles between the resting and activating states remains unchanged.

For case 1, we have applied Huang's ideas to reaction sequence I by use of the relations

$$\alpha_n = f^n \alpha_0 \tag{11}$$

and

$$\beta_n = f^n \beta_0. \tag{12}$$

The factor f is greater than unity and $n = 1$, 2, or 3.

Reaction sequence I, case 1 (Eqs. 11 and 12) was used to simulate the results in Fig. 5. In that experiment, as in all of the experiments reported in this article, gluconate was used as the predominant external anion so that the amount of Q_γ charge would be much larger than that of Q_β charge and, consequently, I_γ would be approximately equal to I_{cm} (Chen and Hui, 1991). In this situation, it seems reasonable to make the approximation that the values of $\bar{V}$, k, and q_{max}/c_m for Q_γ are equal to the parameters of the fitted Boltzmann distribution function in Fig. 5 *B*: $\bar{V} = -48.1$ mV, $k = 6.1$ mV, and $q_{max}/c_m = 29.7$ nC/μF. The value of Q_{max}, the amount of charge expected for a strong depolarization (to −20 to 0 mV), was obtained by multiplication of the value of q_{max}/c_m by the value of C_{app} and by the factor 0.8 to correct for current flow under the Vaseline seals (Table I in Hui and Chandler, 1990). The value of Q_{max} obtained in this manner is ~280 pC.

Although the values of $\bar{V}$ and k determine the value of the ratio α_0/β_0 (Eqs. 9 and 10), they do not determine the functional form of the voltage dependence of the individual rate constants, α_0 and β_0, that is required for a kinetic calculation. The voltage dependence of α_0 can be estimated from the initial values of the I_γ component of I_{cm} at different pulse potentials. Estimates of these initial values (not shown) were better approximated by a constant field voltage dependence for α_0 than by an exponential voltage dependence. The constant field dependence of α_0 can be written,

$$\alpha_0 = B \cdot \frac{y}{1 - \exp(-y)}, \tag{13}$$

in which B is a positive constant and y is given by Eq. 10. Eqs. 9 and 13 can be combined to give β_0,

$$\beta_0 = B \cdot \frac{(-y)}{1 - \exp(y)}, \tag{14}$$

which also has a constant field voltage dependence. A value of 0.005 ms^{-1} was used for B so that the initial theoretical values of I_γ would approximate the experimental estimates.

Fig. 12 shows theoretical I_γ traces calculated for the same voltages shown in Fig. 5 *A*. The value of f was coarsely adjusted so that the ON segments of the theoretical traces would be similar to the humps in the experimental traces; this gave a value of 2.

Although the ON I_γ traces in Fig. 12 are similar to the experimental records in Fig. 5 *A*, the OFF traces are not. They have a large amplitude and brief duration so that, after pulses to $V \geq -44$ mV, the initial values of the tails are off the scale. Short horizontal lines at $I = -12$ nA indicate the period when the current is < -12 nA. The half-width of the OFF tails progressively decreases with increasing pulse potential, as expected from the inequalities $\beta_3 > \beta_2 > \beta_1 > \beta_0$ that follow from Eq.

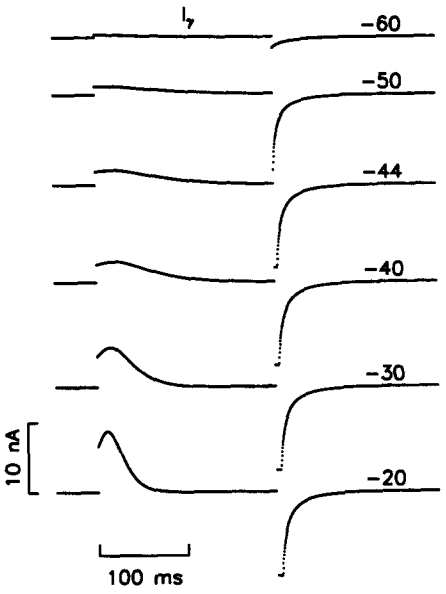

FIGURE 12. Simulations of I_γ based on reaction sequence I, case 1. α_0 and β_0 were calculated from Eqs. 13 and 14, respectively, with $\overline{V} = -48.1$ mV, $k = 6.1$ mV, and $B = 0.005$ ms^{-1}. α_n and β_n were calculated from Eqs. 11 and 12 with $f = 2$. $Q_{max} = 280$ pC. Additional information is given in the text.

12. Similarly, after a pulse to $V = -40$ mV, the OFF half-width progressively decreases with increasing pulse duration (not shown). These effects of the potential and duration of a pulse on the OFF half-width are the opposite of those that were observed experimentally (Figs. 7 *A* and 8 *C*).

Thus, although reaction sequence I, case 1 can generate I_γ humps that are similar to those observed experimentally, it fails to give durations of OFF tails that match the experimental results. A similar conclusion was reached with the original model proposed by Huang (1984), as described in the preceding section.

Case 2: $\alpha_n = f^n \alpha_0$ *and* $\beta_n = f^{-n} \beta_0$. Since increases in OFF half-width accompany increases in either pulse potential (Fig. 7 *A*) or pulse duration (Fig. 8 *C*), it was of interest to explore the possibility that the value of β_n decreases with increasing n. For case 2, calculations were carried out on reaction sequence 1 with α_n given by Eq. 11 and β_n given by

$$\beta_n = f^{-n}\beta_0, \tag{15}$$

with $n = 1$, 2, or 3.

With Eqs. 11 and 15, the theoretical Q_γ vs V curve is determined by four parameters: $\overline{V}$, k, q_{max}/c_m, and f. Similar to the procedure used with case 1, the values of these parameters were determined from a least-squares fit of the theoretical curve to the Q_{cm} vs V data. Because the voltage steepness of the curve depends on k and f in a manner that prevents the reliable estimation of both parameters from Q_{cm} vs V data, the initial calculations were carried out with the value of k set rather arbitrarily to 12 mV. This value corresponds to the e-fold factor for the increase in fiber capacitance that is observed with small depolarizations (Table II in Schneider and Chandler, 1976). It lies within the range of values estimated for Q_β by Hui and Chandler (1990) and used by Pizarro et al. (1991) in their calculations, as de-

scribed above. It is also similar to value of k reported by Melzer et al. (1986) for the charge movement transitions in their three-state, two-transition model of charge movement.

Fig. 13 shows the steady state Q_{cm} vs V data from Fig. 5 *B*. The curve shows the least-squares fit, with gap corrections, of reaction sequence I, case 2 (Eqs. 11 and 15) with the value of k constrained to 12 mV. The fit is clearly good and gives $\overline{V}$ = −31.6 mV, q_{max}/c_m = 30.9 nC/μF, and f = 1.58. As described under case 1, the value of q_{max}/c_m corresponds to a value of ~280 pC for Q_{max}, which is used for the simulations of I_γ described below.

Fits similar to those in Fig. 13, with k constrained to 12 mV, were carried out on the Q_{cm} vs V data from the nine fibers used for Table II. The fits were good and the mean values of the fitted parameters are $\overline{V}$ = −35.4 mV (SEM, 1.1 mV), q_{max}/c_m = 35.5 nC/μF (SEM, 1.4 nC/μF), and f = 1.43 (SEM, 0.04).

Good fits were also obtained with k constrained to 9 or 15 mV. With k = 9 mV, the mean values of the fitted parameters are $\overline{V}$ = −43.4 mV (SEM, 0.9 mV), q_{max}/c_m = 34.4 nC/μF (SEM, 1.3 nC/μF), and f = 1.20 (SEM, 0.03). With k = 15 mV, the mean values of the fitted parameters are $\overline{V}$ = −26.0 mV (SEM, 1.3 mV), q_{max}/c_m = 36.1 nC/μF (SEM, 1.4 nC/μF), and f = 1.64 (SEM, 0.05).

Fig. 14 *A* shows theoretical I_γ traces calculated with the four parameters that determined the theoretical fit to the Q_{cm} vs V data in Fig. 13. The only additional parameter required for the calculations was B, which was given a value of 0.015 ms^{-1} so that the initial values of I_γ at different pulse potentials would approximate the initial values of the hump components in Fig. 5 A. A comparison of Figs. 14 *A* and 5 *A* shows that the theoretical ON humps are less pronounced than the experimental humps and the theoretical OFF tails are more prolonged.

Case 3: $\alpha_n = f'f^n \alpha_0$ *and* $\beta_n = f'f^{-n} \beta_0$. The ON I_γ humps can be made more pronounced by increasing the values of α_n for $n > 0$. If the values of β_n are increased to the same extent, which would make the OFF tails briefer, the equilibrium relation between Q_γ and V would be unchanged and the same values of $\overline{V}$, k,

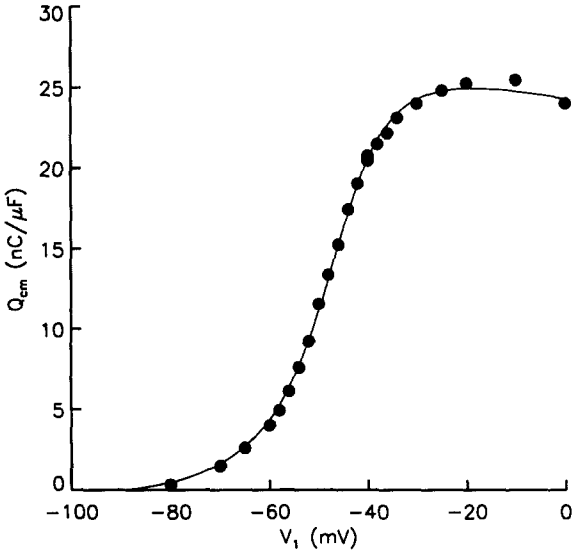

FIGURE 13. Q_{cm} vs V data from Fig. 5 *B* fitted, with gap corrections, with reaction sequence I, case 2. The value of k was constrained to 12 mV and the other parameters were adjusted to give a best least-squares fit: $\overline{V}$ = −31.6 mV, f = 1.58, and q_{max}/c_m = 30.9 nC/μF. Additional information is given in the text.

q_{max}/c_m, and f could be used.

For case 3, the values of α_n and β_n in Eqs. 11 and 15 were each increased by the factor f', which gives

$$\alpha_n = f' f^n \alpha_0, \tag{16}$$

and

$$\beta_n = f' f^{-n} \beta_0, \tag{17}$$

with $n = 1$, 2, or 3.

Fig. 14 *B* shows the traces of I_γ that were calculated in this manner with the same values of $\bar{V}$, k, q_{max}/c_m, f, and B that were used in Fig. 14 *A*. The additional parameter f' was given a value of 2 so that the theoretical I_γ traces would be similar to the I_γ components in the traces in Fig. 5 *A* and in traces from other experiments. The similarity is good. In particular, the ON humps are pronounced, similar to those shown in Figs. 5 *A* and 8 *A* and elsewhere. After large depolarizations, the development of the OFF tails is delayed, similar to that shown in Fig. 7 *B* and in Fig. 8 *A* (where the I_β currents appear to be especially small or absent).

In theory, it should be possible to adjust the values of B and f' so that theoretical traces such as those in Fig. 14 *B* would give least-squares fits of the experimental traces in Fig. 5 *A*. No attempt was made to do this, however, because the information obtained from such fits would be difficult to interpret. Firstly, the experimental traces of I_{cm}, both ON and OFF, contain small contributions from early rapid components. These may arise from I_β or from other rapid currents such as gating

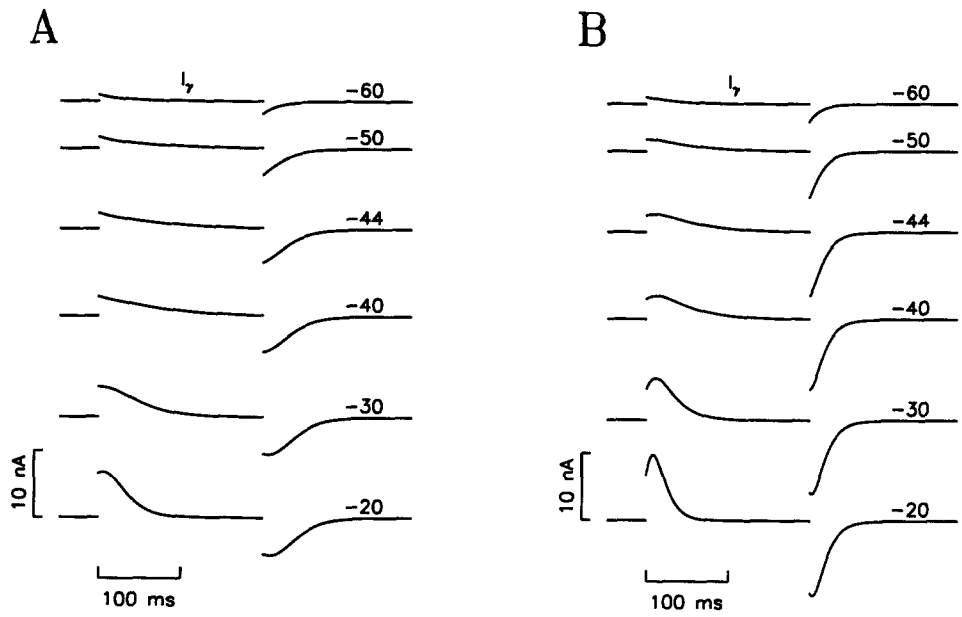

FIGURE 14. Simulations of I_γ based on reaction sequence I, case 2 (A) and case 3 (B). α_0 and β_0 were calculated from Eqs. 13 and 14, respectively, with $\bar{V} = -31.6$ mV, $k = 12$ mV, and $B = 0.015$ ms^{-1}. The values of α_n and β_n were calculated from Eqs. 11 and 15 (*A*) and Eqs. 16 and 17 (*B*) with $f = 1.58$ and $f' = 2$. $Q_{max} = 280$ pC. Additional information is given in the text.

currents from ionic channels located in the surface or tubular membrane. Such rapid components of current were present in all of our experiments except for the fiber used in Fig. 8 from which Q_{cm} vs V data were not obtained. Secondly, the experimental I_{cm} traces are expected to contain contributions from currents that cross fiber membranes under the Vaseline seals; such seal components are present in both the I_{test} and $I_{control}$ records. Fortunately, it is possible to estimate the contributions that these seal currents make to the steady state Q_{cm} vs V data (Hui and Chandler, 1990) so that reliable estimates of equilibrium parameters (such as $\overline{V}$) can be obtained from such data, as was done in Figs. 5 *B* and 13. On the other hand, it would be difficult to estimate the contribution that seal currents make to the time course of I_{cm}. As a result, it would be difficult to estimate their effects on the values of B and f' that would be obtained from least-squares fits of the traces in Fig. 5 *A* with theoretical traces such as those in Fig. 14 *B*.

Fig. 15 *A* shows the half-widths of the theoretical OFF I_γ traces, plotted as a function of pulse potential. The sigmoid relation is qualitatively similar to the experimental relation in Fig. 7 *A*, at least for $V \leq -30$ mV. Fig. 15 *B* shows the half-widths of OFF I_γ after a pulse to −40 mV, plotted against pulse duration. The monotonically increasing relation is similar to that observed experimentally (Fig. 8 *C*).

Although the theoretical results in Fig. 15 are qualitatively similar to the experimental results, three quantitative differences exist. One difference is that the experimental half-widths are briefer than the theoretical half-widths when the pulse potential is more negative than −60 mV (Figs. 7 *A* and 15 *A*) or the pulse duration is brief, 10–20 ms (Figs. 8 *C* and 15 *B*). This is due, at least in part, to the rapid component of I_{cm} that is present in the experimental traces but is not included in the theoretical model of I_γ. Rapid components in I_{cm} might include I_β, ionic channel gating currents, and different relative amounts of seals currents in I_{test} and $I_{control}$.

The two other differences, which are illustrated in the comparison of Figs. 7 *A* and 15 *A*, are more interesting. One difference is that the experimental values of OFF half-width increase more steeply with voltage from −60 to −40 mV than do the theoretical values. Although the steepness of this effect varied somewhat from fiber to fiber, it usually exceeded the steepness of the theoretical points. The other difference is that, in all fibers, the experimental values of OFF half-width progressively increased for $V > -30$ mV whereas the theoretical values reach a plateau level. The experimental increase from −20 to 0 mV is associated with a change in the OFF kinetics of I_{cm} (Fig. 7 *B*) without much change in the amplitude of OFF Q_{cm} (Fig. 5 *B*). This feature of the experimental results is not incorporated into reaction sequence I, case 3 (Eqs. 16 and 17) in which each of the four transitions of x_n to x_{n+1} ($n = 0, 1, 2$, or 3) produces the same amount of charge.

Another problem with the theoretical model is that, in its simplest form, it does not predict a steeply voltage-dependent component of Q_{cm}, as has been observed by Hui and Chandler (1990, 1991) in fibers studied under similar conditions with chloride instead of gluconate as the primary external anion. Their results and our observation of a steep voltage dependence of OFF half-width from −60 to −40 mV suggest that one of the steps in the reaction sequence for charge movement has a small value of k.

These differences between theoretical predictions and experimental results sug-

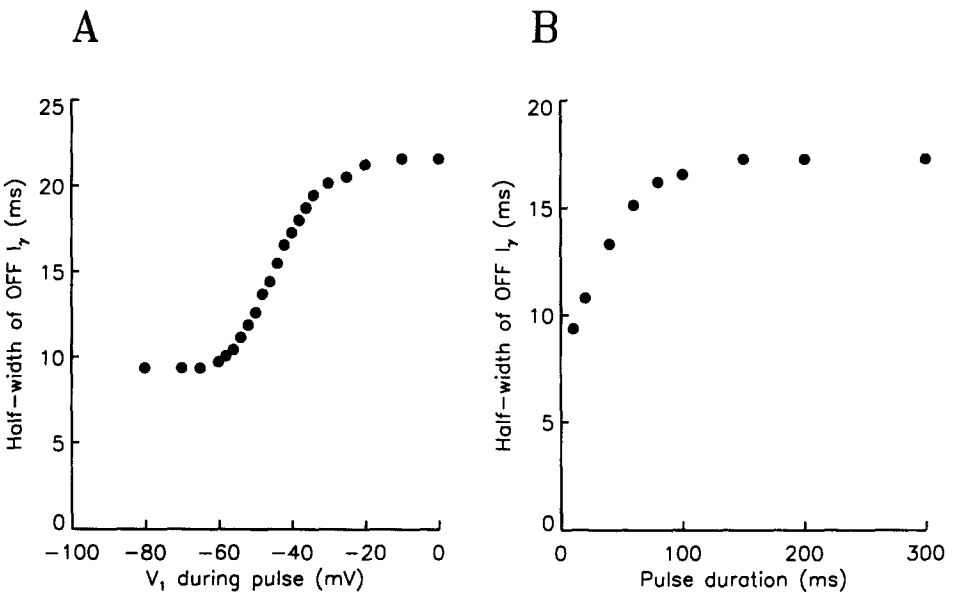

FIGURE 15. Half-width of OFF I_γ plotted as a function of pulse potential (*A*) and pulse duration (*B*). From the simulations illustrated in Fig. 14 *B* and others (not shown) calculated with the same parameters. In *B*, the pulse potential was −40 mV. Additional information is given in the text.

gest that the five-state model of Q_γ, reaction sequence I, case 3, may be too simple. For example, the same value of k may not apply to all of the transitions between different states and/or the number of states may exceed five. This is not surprising since different values of k and as many as 16 states appear to be required to explain the properties of some ionic channels (Sigworth, 1993; Zagotta, Hoshi, and Aldrich, 1994).

The general conclusion of this section is that reaction sequence I, case 3 provides a simple, qualitatively successful model of Q_γ charge. The model has five states and six adjustable parameters: four of the parameters determine the steady state Q_γ vs V relation and two additional parameters are used to calculate I_γ. Although the model fails to provide a quantitative fit to the rather complex relation between OFF half-width and pulse potential (Fig. 7 *A*) and does not explain the steeply voltage-dependent component of Q_{cm} that was observed by Hui and Chandler (1990, 1991), it successfully accounts for most of our experimental observations on I_γ in Ca-depleted fibers. In addition, the model provides an explanation for the voltage dependence of SR Ca release, as described in the following section.

The Steep Voltage Dependence of SR Ca Release Elicited by Small Depolarizations Can Be Explained in Terms of the Model of Q_γ

Since reaction sequence I, case 3 (Eqs. 16 and 17) provides a reliable description of most of the properties of Q_γ, it is important to find out whether it can also account

for the voltage dependence of the activation of SR Ca release. For this purpose, we assume that x_4 represents the activation state of the voltage sensor and that x_0, x_1, x_2, and x_3 represent precursor states. According to the parameters obtained from fits of the Q_{cm} vs V data with reaction sequence I, case 3 (preceding section), the mean steady state values of x_4 at −90 mV with k = 9, 12, and 15 mV are $<2 \times 10^{-5}$, in accord with the upper limit of 10^{-4} estimated in the Appendix.

For small depolarizations, the steady state value of x_4 increases approximately exponentially with potential (not shown). With the parameters used for the theoretical fit in Fig. 13, with k constrained to 12 mV, the steady state value of x_4 increases e-fold every 3.28 mV in the range $0 < x_4 < 0.01$. With k constrained to 9 or 15 mV, the e-fold factor is 2.60 or 3.94 mV, respectively.

e-fold factors were determined within the range $0 < x_4 < 0.01$ in the nine experiments tabulated in Table II, with k = 9, 12, and 15 mV. The mean values are 2.70 mV (SEM, 0.03 mV) with k = 9 mV, 3.39 mV (SEM, 0.03 mV) with k = 12 mV, and 4.07 mV (SEM, 0.03 mV) with k = 15 mV.

Because the fibers used for Table II had been depleted for Ca, it was not possible to determine the voltage dependence of the rate of SR Ca release in those experiments. In another series of experiments, however, carried out under conditions similar to those used here except for the presence of 1.76 mM Ca in the internal solutions, Pape et al. (1995) found that the rate of SR Ca release elicited with small depolarizations increased e-fold every 3.48 mV (SEM, 0.16 mV). This value is similar to the mean e-fold factors of x_4 given in the preceding paragraph, 2.70, 3.39, and 4.07 mV; the difference is significant for k = 9 and 15 mV and is not significant for k = 12 mV.

If, during small depolarizations in fibers equilibrated with 20 mM EGTA, Ca inactivation of Ca release exerts either no effect or the same relative effect at different potentials (Jong, Pape, Baylor, and Chandler, 1995), the e-fold factor for SR Ca release measured by Pape et al. (1995) would be expected to be the same as that for the activation of SR Ca release. In this case, since the e-fold factors of SR Ca release and of x_4 are similar, reaction sequence I, case 3 appears to be able to account for the voltage dependence of the rate of SR Ca release elicited with small depolarizations.

An Explanation for the Occurrence of SR Ca Release in Fibers that Do Not Show I_γ Humps

Several laboratories have simultaneously measured I_{cm} and the changes in myoplasmic free [Ca] that are produced by SR Ca release, starting with the studies of frog muscle by Kovács, Ríos, and Schneider (1979), Rakowski, Best, and James-Kracke (1985), and Melzer et al. (1986). In these and some of the subsequent studies on frog muscle, I_γ humps were either absent or greatly reduced, although SR Ca release was clearly elicited. Similarly, apart from the observation of small I_γ humps in rabbit muscle (Lamb, 1986), prominent I_γ humps are not usually observed in mammalian muscle. Are these observations, which show that SR Ca release can occur in the absence of I_γ humps, consistent with reaction sequence I?

Simon and Hill (1992) studied the kinetics of charge movement and SR Ca re-

lease in frog fibers that did not show I_γ humps; the time course of ON and OFF I_{cm} was approximately exponential. Simon and Hill found that the time course of the rate of release matched that of Q_{cm}^4 and that the relation between the steady state rate of release and voltage matched that of Q_{cm}^4 and voltage. Unfortunately, the comparison between the time courses of Q_{cm}^4 and the rate of SR Ca release is complicated by the fact that, to prevent the development of Ca inactivation of Ca release during their depolarizations, Simon and Hill used prepulses to inactivate most of the release mechanism. Consequently, under the conditions of their experiments, the time course of the rate of SR Ca release is expected to lag the time course of activation by charge movement by ~2 ms, presumably because of the time required for removal of some of the Ca inactivation (Jong et al., 1995).

Simon and Hill (1992) explained their results in terms of activation by four charge movement particles (DHPR's) that have identical properties and are able to move independently of each other. Their model can be represented by reaction sequence I with $\alpha_3 = \alpha_2 = \alpha_1 = \alpha_0$ and $\beta_3 = \beta_2 = \beta_1 = \beta_0$. This is different from the model used for the simulations in Fig. 14 *B* in which the factors f and f', both greater than unity, introduce a substantial interaction among the four particles. Simon and Hill's findings raise the interesting possibility that, under some conditions such as those encountered in our experiments, the four particles in a tetrad may be able to interact and alter the values of the rate constants. Under other conditions, however, such cooperative interactions may not occur. In either case, SR Ca release would be activated when all four particles are in the activating position.

The idea that four charge movement particles can move either independently or as interacting particles is reminiscent of a proposal made by Hui and Chandler (1990) that the Q_β component of charge movement might reflect the movement of a single DHPR and that Q_γ might reflect the movement of groups of four DHPR's. If this is the case, and if the Q_β and Q_γ DHPR's are all located in tetrads, the essential difference between Q_β and Q_γ might depend on whether cooperative interactions can occur among the four DHPR's in a tetrad. Since such interactions might depend on the species of animal or some of the experimental conditions, the degree of cooperativity, and consequently the prominence of I_γ humps, might vary from study to study.

Is the Effect of SR Ca on the Time Course of ON I_{cm} Due to SR Ca Content or Release or Some Related Event?

Although our experiments show that neither the presence of Ca inside the SR nor the movement of Ca from the SR into myoplasm is the fundamental cause of Q_γ, it is clear from experiments such as the one illustrated in Fig. 2 that the ON kinetics of I_γ is affected in some way by SR Ca. This effect, first demonstrated by Csernoch et al., (1991), García et al. (1991), Szucs et al. (1991), and Pizarro et al. (1991), can be described as an increase in the value of k_{app} (Figs. 9–11). If this increase is due to a direct effect of SR Ca content, the results in columns 3 and 4 in Table III show that the sensitivity of k_{app} to SR Ca content depends on pulse potential: between −50 and −30 mV, the value of $[Ca_{SR}]_{R,1/2}$ changes severalfold. Although this doesn't rule out a direct effect of SR Ca content on k_{app}, additional reasons are re-

quired to explain why the effect depends on the voltage across the external (surface and tubular) membranes and why it develops with a delay (Fig. 10).

On the other hand, if the increase in k_{app} depends on the rate of SR Ca release, the sensitivity of the effect appears to be independent of potential: between −50 and −30 mV, the value of $d\Delta[Ca_T]/dt_{1/2}$ is relatively constant, with mean values at different potentials that vary between 1.2 and 1.4 μM/ms (column 6 in Table III). This is clearly consistent with the idea that, in these experiments, k_{app} is influenced by the rate of SR Ca release or some related event. This interpretation is also consistent with the observation that the time course of the increase in ON k_{app} roughly corresponds to the time course of the rate of SR Ca release (Fig. 10).

An important example of an event related to SR Ca release is the increase in free [Ca] that is expected to occur in the myoplasm. Pape et al. (1995) showed that, in fibers equilibrated with 20 mM EGTA such as those used in our experiments, this increase is expected to be restricted to distances within a few hundred nanometers of the release sites. Furthermore, at any location within this region, the time course of the increase in free [Ca] is expected to be similar to that of $d\Delta[Ca_T]/dt$, at least for the small amounts of SR Ca release encountered in our experiments, and the amplitude of the increase is expected to depend inversely on distance from the release sites. Thus, a plausible explanation of the acceleratory effect of SR Ca on k_{app} (or, more generally, on the ON kinetics of I_γ) is that it is caused by the increase in free [Ca] that occurs in the myoplasm near the release sites during the period of SR Ca release.

Possible Explanations for the Effect of SR Ca on k_{app}

Although SR Ca does not cause Q_γ, it can exert an acceleratory effect on the ON kinetics of I_γ, perhaps by increasing the value of myoplasmic free [Ca] near the release sites (preceding section). This could be due to a specific action of myoplasmic Ca, such as Ca binding to a site associated with the DHPR, the ryanodine receptor (RyR), or some intermediate protein that facilitates the interaction between the DHPR and the RyR. After Ca is bound to this site, the activation energy associated with a particular charge movement transition(s) might be reduced, thereby increasing k_{app}. Our results provide no information about which protein might contain such a site or whether such a site is also involved in other actions of Ca, such as Ca-induced Ca release or Ca inactivation of Ca release.

Another explanation for the effect of SR Ca on k_{app} is provided by the surface potential hypothesis. According to this idea (see Introduction), Ca released from the SR produces an elevation in myoplasmic free [Ca] next to the tubular membrane. This produces a change in surface potential that leads to a shift in the Q_γ vs V relation to more negative potentials, thereby increasing k_{app}. This idea is similar to that used by Pizarro et al. (1991) to explain the origin of Q_γ in terms of a shift in the Q_β vs V relation produced by SR Ca release, as described in the Introduction. Because our results show that Q_γ represents a distinct species or transition of intramembranous charge, any effect of surface potential on k_{app} would be expected to be due to an effect on the Q_γ vs V, and not the Q_β vs V, relation.

The surface potential hypothesis is consistent with our experimental results on

the effect of SR Ca on k_{app}. In particular, the values of $[k_{app}/k_{app,0} - 1]_{max}$ in columns 3 and 5 in Table III are largest at −50 mV and smallest at −30 mV, showing that the amplitude of the acceleratory effect of SR Ca on k_{app} depends rather markedly on pulse potential. Because the value of $\overline{V}$ is close to −50 mV (column 4 in Table II), the effect of SR Ca on k_{app} is most marked at voltages where a given shift of the Q_{cm} vs V curve along the voltage axis is expected to produce the largest change in the steady state value of Q_{cm}. Such a correlation is expected from the surface potential hypothesis.

Pizarro et al. (1991) and Shirokova et al. (1994) sometimes observed a negative phase in the ON I_{cm} a few tens of milliseconds after depolarization, after completion of the I_γ hump. This was only observed during pulses within a narrow range of voltages. Its presence may be enhanced by the use of slack length fibers, small conditioning depolarizations applied prior to the test pulses, and large SR Ca contents. Pizarro et al. (1991) and Shirokova et al. (1994) explained the negative phase in the ON I_{cm} in terms of the surface potential hypothesis. During SR Ca release, they reasoned, the Q_{cm} vs V relation is shifted to more negative potentials, which favors the movement of additional charge or positive I_{cm}, as described above. After Ca release is over but before the pulse is terminated, the surface potential and consequently the steady state Q_{cm} vs V relation return to their respective resting conditions. This favors the movement of charge in the negative direction and, under optimal conditions, a negative I_{cm} would be observed. Thus, a negative phase of I_{cm} is consistent with the surface potential hypothesis.

Although the surface potential hypothesis is an attractive explanation for the effects of SR Ca on k_{app} that are reported in this article, it is important to point out that a negative phase in the ON I_{cm} has never been observed by Huang (1994*a*), by Hui and Chen (1994), or by us, perhaps because the conditions required for its demonstration were not met. Although these negative findings provide no direct support for the hypothesis, they do not rule it out.

APPENDIX

Ríos et al. (1993) introduced a model to explain the effects of perchlorate on charge movement and SR Ca release in frog skeletal muscle. These effects include an exaggeration of I_γ humps, a shift of the Q_{cm} vs V curve to more negative potentials, an increase in the steepness of the Q_{cm} vs V curve, and a shift in the relation between the rate of SR Ca release and V to more negative potentials (Lüttgau, Gottschalk, Kovács, and Fuxreiter, 1983; González and Ríos, 1993; Ríos et al., 1993). In their model, a single SR Ca channel is activated by four identical charge movement particles, presumably DHPR's. Since their model appears to explain the effects of perchlorate on charge movement and SR Ca release, we wanted to find out whether the same model could account for the properties of charge movement that we observed in Ca-depleted fibers, particularly the appearance of prominent I_γ humps. This Appendix describes our attempts to do this. The most interesting result is that pronounced I_γ humps cannot be calculated with this model, at least in its original form, with any set of parameters that is consistent with both the steady state Q_{cm} vs V data and the small rate of Ca flux that is expected from the resting SR.

General Description of the Model Proposed by Ríos et al. (1993)

Marks and Jones (1992) introduced a 10-state model, with five closed and five open states, to explain the gating behavior of a single L-type calcium channel in the presence and absence of dihydropyridine agonists. This model was adapted by Ríos et al. (1993) to describe the activation of a single SR Ca channel by four charge movement particles. According to the model, an SR Ca channel is either closed or open, and each charge particle is in either a resting or an activating state. In this situation, there are five different closed states of the SR Ca channel-voltage sensor complex according to the number of charge particles, n, that are in the activating state. These states are denoted by C_n with $n = 0$, 1, 2, 3, or 4. Similarly, there are five open states of the complex, denoted by O_n. Transitions among the different states are assumed to occur according to the reaction sequence

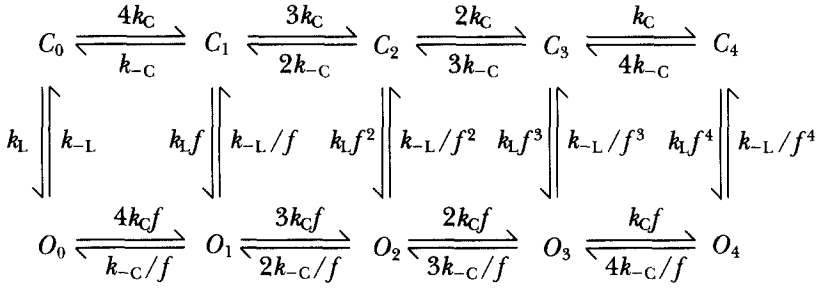

REACTION SEQUENCE AI

The top row shows the different closed states of the system, with k_C and k_{-C} representing, respectively, the forward and backward rate constants for transitions between adjacent states. These rate constants depend on voltage according to

$$k_C = 0.5\alpha \exp[(V - \overline{V})/8K] \tag{A1}$$

and

$$k_{-C} = 0.5\alpha \exp[-(V - \overline{V})/8K]. \tag{A2}$$

Eqs. A1 and A2 are the same as Eqs. 2 and 3 in Ríos et al. (1993). The voltage dependence of k_C/k_{-C} in Eqs. A1 and A2 is the same as that expected from k in Eq. 1 if $k = 4K$.

The bottom row in reaction sequence AI shows the different open states of the system, with the forward and backward rate constants k_C and k_{-C} multiplied by f and $1/f$, respectively. The values of f and of k_L and k_{-L}, the rate constants for vertical transitions between closed and open states, are assumed to be constant and independent of V. In the cases considered by Ríos et al. (1993) and in this Appendix, the value of f is greater than unity. The symbols denoting the various parameters in reaction sequence AI are the same as those in Fig. 10 in Ríos et al. (1993) except that f replaces $1/f$.

The probability that an SR Ca channel is open, P_o, is given by

$$P_o = \frac{o_0 + o_1 + o_2 + o_3 + o_4}{c_0 + c_1 + c_2 + c_3 + c_4 + o_0 + o_1 + o_2 + o_3 + o_4}. \quad \text{(A3)}$$

In Eq. A3, c_n and o_n, with $n = 0$ to 4, denote the probabilities that the SR Ca channel is in states C_n and O_n, respectively.

With reaction sequence AI, the theoretical Q_{cm} vs V curve is determined by five parameters: $\bar{V}$, K, q_{max}/c_m, f, and k_L/k_{-L}. The time course of I_{cm} is determined by these five parameters plus two additional parameters, α and k_L.

Large Values of f and k_L/k_{-L} Favor the Appearance of Humps

In their calculations of I_{cm} with reaction sequence AI, Ríos et al. (1993) showed that it was possible to simulate small Q_γ humps. These are not nearly as pronounced, however, as those observed in our experiments, even after Ca depletion (Figs. 5 *A*, 6 *B*, and 8 *A*). For this reason, it was important to find out which parameters in reaction sequence AI contribute to the production of humps so that they could be adjusted to make the theoretical humps as pronounced as possible.

If the value of k_L in reaction sequence AI were zero and only the C_n states were allowed to be occupied, the equilibrium Q_{cm} vs V relation would be given by the Boltzmann distribution function, Eq. 1 with $k = 4K$, and the time course of I_{cm} during a depolarizing voltage step would be given by a single decreasing exponential function, without any humps. The only way to get humps with reaction sequence AI is for transitions to occur from C_n to O_n so that the apparent forward rate constant can be increased from k_C to $k_C f$ and the apparent backward rate constant can be decreased from k_{-C} to k_{-C}/f. Since large values of f and k_L/k_{-L} favor transitions from C_n to O_n, they would be expected to favor the production of humps. This expectation was validated in the calculations described below.

The Resting Value of P_o Is Expected to Be $\leq 10^{-4}$, Which Restricts k_L/k_{-L} to Small Values

An upper limit can be placed on the resting value of P_o by taking the ratio of an upper limit of the resting rate of SR Ca release and a lower limit of the maximal rate of SR Ca release.

An upper limit of the resting rate of SR Ca release can be determined from the resting rate of lactate production in anaerobic frog muscle, as described by Baylor, Chandler, and Marshall (1983). The essential assumptions required for this estimate are that (*a*) the Ca content of the SR is maintained constant so that the resting Ca efflux is equal to the rate of reaccumulation by the SR Ca pump, (*b*) all of the ATP produced by glycolysis is used by the SR Ca pump, and (*c*) the SR Ca pump operates with a stoichiometry of 2 Ca per ATP. With these assumptions, the resting rate of lactate production determined by DeFuria and Kushmerick (1977) gives an upper limit of 0.009 μM/ms for the resting rate of SR Ca release, which can occur through SR Ca channels as well as other pathways.

The actual value of the resting rate of SR Ca release in the fibers used in this arti-

cle may have been much smaller than 0.009 μM/ms. After a 57–78 min stimulation-free period of equilibration with a Ca-free external solution and a Ca-free internal solution that contained 20 mM EGTA, the SR contained 839–1,698 μM Ca. Although it was not possible in these experiments to determine the initial value of SR Ca content before equilibration with EGTA, it seems unlikely that it could have been much larger than 2–3 mM, which is observed in fibers equilibrated with the same internal solution but with 1.76 mM Ca (Fig. 9 in Pape et al., 1995). This suggests that the decrease in $[Ca_{SR}]_R$ during the period of equilibration was no more than 1–2 mM. If the SR Ca pump was unable to reaccumulate the Ca that left the SR and became bound by EGTA, the resting Ca efflux averaged over the period of equilibration was probably no more than 1–2 mM/h or 0.0003–0.0006 μM/ms.

A lower limit of the maximal rate of SR Ca release can be obtained from experiments carried out under conditions similar to those used here except for the presence of 1.76 mM Ca (with 20 mM EGTA) in the internal solution. In these experiments, the peak rate of SR Ca release was of the order of 100 μM/ms (Pape et al., 1995). Since the peak rate of release may have been attenuated by Ca inactivation of Ca release (Jong et al., 1995), 100 μM/ms represents a lower limit of the maximal rate of SR Ca release.

The values 0.009 μM/ms for the resting rate of SR Ca release (upper limit) and 100 μM/ms for the peak rate of release (lower limit) indicate that the resting value of P_o is small and does not exceed 10^{-4}; in fact, the information in the preceding two paragraphs indicates that it may actually be much smaller than 10^{-4}. In terms of reaction sequence AI, this means that the value of k_L/k_{-L}, which determines the equilibrium distribution between states C_0 and O_0, cannot exceed 10^{-4}. In many of the examples described below, however, in which the resting occupancy of states other than C_0 and O_0 must be taken into account, an upper limit of 10^{-4} for the resting value of P_o requires a value for k_L/k_{-L} that is $\ll 10^{-4}$. It should be pointed out that the requirement that the resting value of P_o should not exceed 10^{-4} was met in all of the simulations reported in Table I in Ríos et al. (1993), in which the value of P_o at −90 mV was $\leq 0.7 \times 10^{-4}$.

Steady State Q_{cm} vs V Relation

The results in Fig. 5 were analyzed with reaction sequence AI in much the same way that is done in the Discussion with reaction sequence I, as illustrated in Figs. 13–14. First, the steady state Q_{cm} vs V data in Fig. 5 B were least-squares fitted with reaction sequence AI to give values for the five parameters $\bar{V}$, K, q_{max}/c_m, f, and k_L/k_{-L}, as described in this section. Then, the parameters α and k_L were adjusted to give I_{cm} waveforms that best resembled those in Fig. 5 A, as described in the following section.

Because the Q_{cm} vs V data in our experiments are well fitted by a single Boltzmann distribution function (Fig. 5 B), with three adjustable parameters, it is not surprising that reliable estimates of all five parameters in reaction sequence AI cannot be obtained from Q_{cm} vs V data alone. The main reason is that the steepness of the theoretical Q_{cm} vs V curve is determined by the three parameters K, f, and k_L/k_{-L}: an increase in steepness of the curve is produced by a decrease in K or an increase in f or k_L/k_{-L}. In the calculations described in this section, values were assigned to

K and k_L/k_{-L} and then the values of $\bar{V}$, q_{max}/c_m, and f were adjusted to give a least-squares fit to the Q_{cm} vs V data.

The values assigned to K were 2, 3, 4, and 5 mV (which correspond to k = 8, 12, 16, and 20 mV in Eq. 1). These span the range in Table I in Ríos et al. (1993), K = 3.2-4.5 mV. For each value of K, the value of k_L/k_{-L} was varied between 10^{-8} and the upper limit 10^{-4}, which was estimated in the preceding section. Calculations of I_{cm} (described in the following section) showed that, for each value of K, the most pronounced humps were obtained with the largest values of k_L/k_{-L} and, for each value of k_L/k_{-L}, with a large value of k_L, 0.1 ms^{-1} (larger values made no discernible difference).

Fig. 16 A shows the Q_{cm} vs V data from Fig. 5 B fitted with reaction sequence AI, with gap corrections. The value of K was constrained to 4 mV and the value of k_L/k_{-L} was increased to the maximal value consistent with a resting value of P_o no greater than $\sim 10^{-4}$ (preceding section); this gave a value of 10^{-6} for k_L/k_{-L}, which gives $P_o = 1.4 \times 10^{-4}$ at −90 mV, the resting potential in our experiments. The fitted parameters are $\bar{V}$ = −27.9 mV, q_{max}/c_m = 31.9 nC/μF, and f = 11.1. The fit in Fig. 16 A is clearly good and is representative of fits obtained with other combinations of K and k_L/k_{-L}.

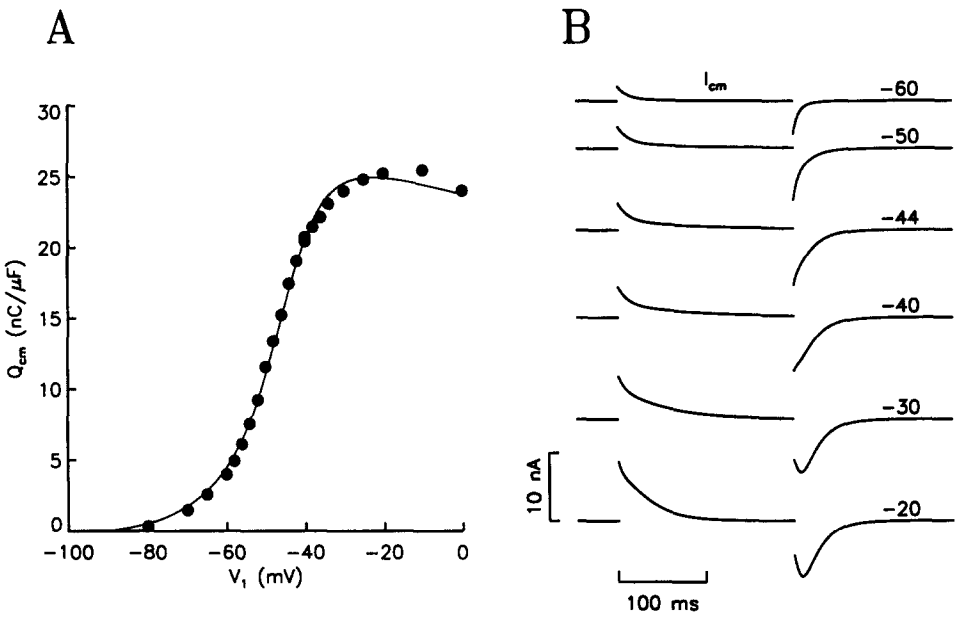

FIGURE 16. Calculations with reaction sequence AI with $P_o = 10^{-4}$ at −90 mV. (*A*) The circles show the Q_{cm} vs V data from Fig. 5 *B*. The theoretical curve was fitted to the data with the constrained parameters K = 4 mV and $k_L/k_{-L} = 10^{-6}$; the fitted parameters are Q_{max}/c_m = 31.9 nC/μF, $\bar{V}$ = −27.9 mV, and f = 11.1. (*B*) I_{cm} was calculated with these parameters and Q_{max} = 280 pC (obtained from the value of q_{max}/c_m as described in the text in connection with Fig. 12); α = 0.05 ms^{-1} and k_L = 0.1 ms^{-1}. Additional information is given in the Appendix.

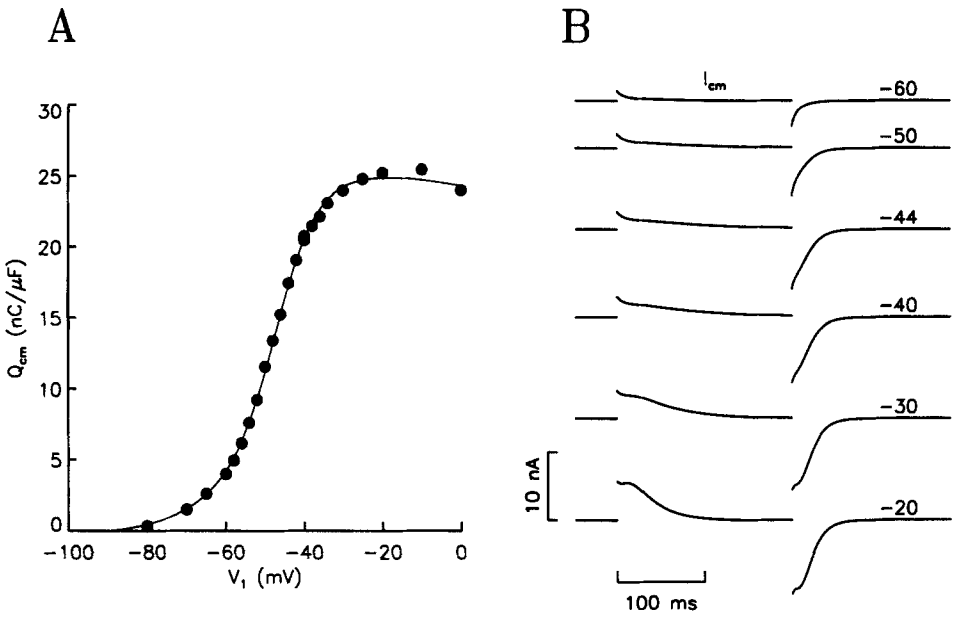

FIGURE 17. Calculations with reaction sequence AI with P_o = 0.0037 at −90 mV. (*A*) The circles show the Q_{cm} vs V data from Fig. 5 *B*. The theoretical curve was fitted to the data with the constrained parameters K = 4 mV and $k_L/k_{-L} = 10^{-3}$; the fitted parameters are Q_{max}/c_m = 31.1 nC/μF, $\bar{V}$ = −13.7 mV, and f = 6.9. (*B*) I_{cm} was calculated with these parameters and Q_{max} = 280 pC (obtained from the value of q_{max}/c_m as described in the text in connection with Fig. 12); α = 0.05 ms^{-1} and k_L = 0.1 ms^{-1}. Additional information is given in the Appendix.

The value of P_o was calculated at different values of V with the parameters used for the theoretical Q_{cm} vs V curve in Fig. 16 A. For small depolarizations, the value of P_o increases *e*-fold every 4.61 mV. *e*-fold factors were also determined with other combinations of K and k_L/k_{-L} that gave a value of about 10^{-4} for P_o at −90 mV. For K = 2 and 3 mV, the *e*-fold factors were 3.71 and 4.39 mV, respectively. These values of the theoretical *e*-fold factor for the rate of SR Ca release during small depolarizations are just slightly larger than the mean experimental value reported by Pape et al. (1995), 3.48 mV.

Simulations of I_{cm} with Depolarizing Voltage Pulses

Fig. 16 B shows theoretical I_{cm} traces that were calculated with the parameters used for the Q_{cm} vs V fit in Fig. 16 A. The values of the other two parameters, α = 0.05 ms^{-1} and k_L = 0.1 ms^{-1}, were chosen so that the initial values of I_{cm} would roughly match the experimental values (α) and the humps would be as pronounced as possible (k_L). Although there is a suggestion of humps in the ON components, they are not conspicuous and are much less pronounced than those in Fig. 5 A.

Calculations similar to those in Fig. 16 *A* and *B* were also carried out with K = 2, 3, and 5 mV and with values of k_L/k_{-L} that gave values of $\sim 10^{-4}$ for the value of P_o at −90 mV. In all cases, the humps were no more conspicuous than those in Fig. 16 *B*.

The only way to obtain pronounced humps with reaction sequence AI, at least in its original form, is to increase k_L/k_{-L} to values that predict resting values of P_o that are unrealistically large. Fig. 17 shows an example, plotted with the same format used for Fig. 16. The theoretical curve in Fig. 17 *A* was obtained with the values of K and k_L/k_{-L} constrained to 4 mV and 10^{-3}, respectively. The fitted parameters were $\overline{V} = -13.7$ mV, $q_{max}/c_m = 31.1$ nC/μF, and $f = 6.9$. The traces in Fig. 17 *B*, calculated with $\alpha = 0.05$ ms^{-1} and $k_L = 0.1$ ms^{-1} (the same values used in Fig. 16 *B*), show well developed humps, although they are still not quite as pronounced as those observed in our experiments on Ca-depleted fibers (Figs. 5 *A*, 6 *B*, and 8 *A*). The value of k_L/k_{-L} that was used for the simulations, 10^{-3}, is unrealistically large, however. It predicts a value of 0.0037 for P_o at −90 mV, which is 37 times the maximal value of 10^{-4} estimated above.

The general conclusion of this section and the Appendix is that pronounced Q_γ humps cannot be calculated with reaction sequence AI, at least in its original form, with any set of parameters that fits the steady state Q_{cm} vs V data and also satisfies the condition that $P_o \leq 10^{-4}$ at −90 mV.

We thank the staff of the Biomedical Instrumentation Laboratory of the Yale Department of Cellular and Molecular Physiology for help with the design and construction of equipment. We thank Dr. Fred Sigworth for giving us a copy of his modified Simplex program for curve fitting. We thank Dr. Steve Baylor for many helpful discussions. We are grateful to him and Dr. Stephen Hollingworth for reading the manuscript and providing useful criticism.

This work was supported by U.S. Public Health Service grant AM-37643.

Original version received 24 March 1995 and accepted version received 8 May 1995.

REFERENCES

Adrian, R. H., and W. Almers. 1976. Charge movement in the membrane of striated muscle. *Journal of Physiology.* 254:339–360.

Adrian, R. H., and C. L.-H. Huang. 1984. Experimental analysis of the relationship between charge components in skeletal muscle of *Rana temporaria*. *Journal of Physiology.* 353:419–434.

Adrian, R. H., and A. Peres. 1977. A 'gating' signal for the potassium channel? *Nature.* 267:800–804.

Adrian, R. H., and A. Peres. 1979. Charge movement and membrane capacity in frog muscle. *Journal of Physiology.* 289:83–97.

Almers, W. 1978. Gating currents and charge movements in excitable membranes. *Review of Physiological and Biochemical Pharmacology.* 82:96–190.

Baylor, S. M., W. K. Chandler, and M. W. Marshall. 1983. Sarcoplasmic reticulum calcium release in frog skeletal muscle fibres estimated from arsenazo III calcium transients. *Journal of Physiology.* 344: 625–666.

Bezanilla, F., and E. Stefani. 1994. Voltage-dependent gating of ionic channels. *Annual Review of Biophysics and Biomolecular Structure.* 23:819–846.

Block, B. A., T. Imagawa, K. P. Campbell, and C. Franzini- Armstrong. 1988. Structural evidence for direct interaction between the molecular components of the transverse tubule/sarcoplasmic reticulum junction in skeletal muscle. *Journal of Cell Biology.* 107:2587–2600.

Chandler, W. K., and C. S. Hui. 1990. Membrane capacitance in frog cut twitch fibers mounted in a double Vaseline-gap chamber. *Journal of General Physiology.* 96:225–256.

Chandler, W. K., R. F. Rakowski, and M. F. Schneider. 1976. A nonlinear voltage dependent charge movement in frog skeletal muscle. *Journal of Physiology.* 254:245–283.

Chen, W., and C. S. Hui, 1991. Gluconate suppresses Q_β more effectively than Q_γ in frog cut twitch fibers. *Biophysical Journal.* 59:543*a*. (Abstr.)

Colquhoun, D. 1971. Lectures on Biostatistics. Oxford University Press, Oxford, UK. 425 pp.

Colquhoun, D., and F. J. Sigworth. 1983. Fitting and statistical analysis of single-channel records. *In* Single-Channel Recording. B. Sakmann and E. Neher, editors. Plenum Publishing Corp., New York. 191–263.

Csernoch, L., G. Pizarro, I. Uribe, M. Rodriguez, and E. Ríos. 1991. Interfering with calcium release suppresses I_γ, the "hump" component of intramembranous charge movement in skeletal muscle. *Journal of General Physiology.* 97:845–884.

DeFuria, R. F., and M. J. Kushmerick. 1977. ATP utilization associated with recovery metabolism in anaerobic frog muscle. *American Journal of Physiology.* 232:C30–C36.

Garcia, J., G. Pizarro, E. Ríos, and E. Stefani. 1991. Effect of the calcium buffer EGTA on the "hump" component of charge movement in skeletal muscle. *Journal of General Physiology.* 97:885–896.

González, A., and E. Ríos. 1993. Perchlorate enhances transmission in skeletal muscle excitation-contraction coupling. *Journal of General Physiology.* 102:373–421.

Hille, B., and D. T. Campbell. 1976. An improved Vaseline gap voltage clamp for skeletal muscle fibers. *Journal of General Physiology.* 67:265–293.

Horowicz, P., and M. F. Schneider. 1981. Membrane charge moved at contraction thresholds in skeletal muscle fibres. *Journal of Physiology.* 314:595–633.

Huang, C. L.-H. 1982. Pharmacological separation of charge movement components in frog skeletal muscle. *Journal of Physiology.* 324:375–387.

Huang, C. L.-H. 1983. Experimental analysis of alternative models of charge movement in frog skeletal muscle. *Journal of Physiology.* 336:527–543.

Huang, C. L.-H. 1984. Analysis of 'off' tails of intramembrane charge movements in skeletal muscle of *Rana temporaria*. *Journal of Physiology.* 356:375–390.

Huang, C. L.-H. 1986. The differential effects of twitch potentiators on charge movements in frog skeletal muscle. *Journal of Physiology.* 380:17–33.

Huang, C. L.-H. 1994*a*. Charge conservation in intact frog skeletal muscle fibres in gluconate-containing solutions. *Journal of Physiology.* 474:161–171.

Huang, C. L.-H. 1994*b*. Kinetic separation of charge movement components in intact frog skeletal muscle. *Journal of Physiology.* 481:357–369.

Huang, C. L.-H. and L. D. Peachey. 1989. Anatomical distribution of voltage-dependent membrane capacitance in frog skeletal muscle fibers. *Journal of General Physiology.* 93:565–584.

Hui, C. S. 1983. Differential properties of two charge components in frog skeletal muscle. *Journal of Physiology.* 337:531–552.

Hui, C. S. and, W. K. Chandler. 1990. Intramembranous charge movement in frog cut twitch fibers mounted in a double Vaseline-gap chamber. *Journal of General Physiology.* 96:257–297.

Hui, C. S., and W. K. Chandler. 1991. Q_β and Q_γ components of intramembranous charge movement in frog cut twitch fibers. *Journal of General Physiology.* 98:429–464.

Hui, C. S., and W. Chen. 1994. Evidence for the non-existence of a negative phase in the hump charge movement component (I_γ) in *Rana temporaria*. *Journal of Physiology.* 474:275–282.

Irving, M., J. Maylie, N. L. Sizto, and W. K. Chandler. 1987. Passive electrical and intrinsic optical properties of cut frog twitch fibres. *Journal of General Physiology.* 89:1–40.

Jong, D.-S., P. C. Pape, S. M. Baylor, and W. K. Chandler. 1995. Calcium inactivation of calcium release in frog cut muscle fibers that contain millimolar EGTA or fura-2. *Journal of General Physiology.* 106:337–388.

Jong, D.-S., P. C. Pape, and W. K. Chandler. 1992. Effects of sarcoplasmic reticulum (SR) calcium depletion on intramembranous charge movement in frog cut muscle fibers. *Biophysical Journal.* 61: A130. (Abstr.)

Kovacs, L., E. Rios, and M. F. Schneider. 1979. Calcium transients and intramembrane charge movement in skeletal muscle fibres. *Nature.* 279:391–396.

Kovacs, L., E. Rios, and M. F. Schneider. 1983. Measurement and modification of free calcium transients in frog skeletal muscle fibres by a metallochromic indicator dye. *Journal of Physiology.* 343: 161–196.

Lamb, G. D. 1986. Asymmetric charge movement in contracting muscle fibres in the rabbit. *Journal of Physiology.* 376:63–83.

Lüttgau, H. C., G. Gottschalk, L. Kovács, and M. Fuxreiter. 1983. How perchlorate improves excitation-contraction coupling in skeletal muscle fibers. *Biophysical Journal.* 41:247–249.

Marks, T. N., and S. W. Jones. 1992. Calcium currents in the A7r5 smooth muscle-derived cell line. An allosteric model for calcium channel activation and dihydropyridine agonist action. *Journal of General Physiology.* 99:367–390.

Melzer, W., M. F. Schneider, B. J. Simon, and G. Szucs. 1986. Intramembrane charge movement and calcium release in frog skeletal muscle. *Journal of Physiology.* 373:481–511.

Pape, P. C., D.-S. Jong, and W. K. Chandler. 1992. Effects of sarcoplasmic reticulum (SR) calcium loading on intramembranous charge movement in frog cut muscle fibers. *Biophysical Journal.* 61: A130. (Abstr.)

Pape, P. C., D.-S. Jong, and W. K. Chandler. 1995. Calcium release and its voltage dependence in frog cut muscle fibers equilibrated with 20 mM EGTA. *Journal of General Physiology.* 106:259–336.

Pape, P. C., D.-S. Jong, and W. K. Chandler. 1996. A slow component of intramembranous charge movement during sarcoplasmic reticulum calcium release in frog cut muscle fibers. *Journal of General Physiology.* In press.

Pizarro, G., L. Csernoch, I. Uribe, M. Rodriguez, and E. Rios. 1991. The relationship between Q_γ and Ca release from the sarcoplasmic reticulum in skeletal muscle. *Journal of General Physiology.* 97:913–947.

Rakowski, R. F., P. M. Best, and M. R. James-Kracke. 1985. Voltage dependence of membrane charge movement and calcium release in frog skeletal muscle fibres. *Journal of Muscle Research and Cell Motility.* 6:403–433.

Ríos, E., and G. Brum. 1987. Involvement of dihydropyridine receptors in excitation-contraction coupling in skeletal muscle. *Nature.* 325:717–720.

Ríos, E., M. Karhanek, J. Ma, and A. González. 1993. An allosteric model of the molecular interactions of excitation-contraction coupling in skeletal muscle. *Journal of General Physiology.* 102:449–481.

Rios, E., and G. Pizarro. 1991. Voltage sensor of excitation-contraction coupling in skeletal muscle. *Physiological Reviews.* 71:849–908.

Schneider, M. F., and W. K. Chandler. 1973. Voltage-dependent charge movement in skeletal muscle: a possible step in excitation-contraction coupling. *Nature.* 242:244–246.

Schneider, M. F., and W. K. Chandler. 1976. Effects of membrane potential on the capacitance of skeletal muscle fibers. *Journal of General Physiology.* 67:125–163.

Schneider, M. F. 1994. Control of calcium release in functioning skeletal muscle fibers. *Annual Reviews of Physiology.* 56:463–484.

Shirokova, N., G. Pizarro, and E. Ríos. 1994. A damped oscillation in the intramembranous charge movement and calcium release flux of frog skeletal muscle fibers. *Journal of General Physiology.* 104: 449–477.

Sigworth, F. J. 1993. Voltage gating of ion channels. *Quarterly Reviews of Biophysics.* 27:1–40.

Simon, B. J., and D. A. Hill. 1992. Charge movement and SR calcium release in frog skeletal muscle can be related by a Hodgkin-Huxley model with four gating particles. *Biophysical Journal.* 61:1109–1116.

Szucs, G., L. Csernoch, J. Magyar, and L. Kovacs. 1991. Contraction threshold and the "hump" component of charge movement in frog skeletal muscle. *Journal of General Physiology.* 97:897–911.

Tanabe, T., K. G. Beam, J. A. Powell, and S. Numa. 1988. Restoration of excitation-contraction coupling and slow calcium current in dysgenic muscle by dihydropyridine receptor complementary DNA. *Nature.* 336:134–139.

Vergara, J., and C. Caputo. 1983. Effects of tetracaine on charge movements and calcium signals in frog skeletal muscle fibres. *Proceedings of the National Academy of Sciences, USA.* 80:1477–1481.

Zagotta, W. N., T. Hoshi, and R. W. Aldrich. 1994. *Shaker* potassium channel gating III: evaluation of kinetic models for activation. *Journal of General Physiology.* 103:321–362.